Recent Advances in Vertical Drains and Vacuum Preloading for Soft Ground Stabilisation

Développements récents dans l'amélioration des terrains mous par drains verticaux et préchargement par le vide

Buddhima Indraratna
Centre for Geomechanics and Railway Engineering, University of Wollongong, Australia, indra@uow.edu.au

ABSTRACT: Much of the world's essential infrastructure is built along congested coastal belts that are composed of weak and highly compressible soils to significant depths. Soft alluvial and marine clay deposits have very low bearing capacity and excessive settlement characteristics. This has design and maintenance implications for tall structures, large commercial buildings, as well as port and transport infrastructure constructed on such poor soils. Stabilising these very soft deposits is essential before commencing construction of infrastructure. A system of vertical drains combined with vacuum pressure and surcharge preloading has become an efficient and cost effective ground improvement option. This technique accelerates consolidation by promoting rapid radial flow which decreases the excess pore pressure while increasing the effective stress. This 4th Louis Menard lecture presents an overview of the theoretical and practical developments of soft ground improvement via prefabricated vertical drains, PVD (including natural fibre drains) and vacuum preloading, with application to selected case studies in Australia.

RÉSUMÉ: La plupart des infrastructures dans le monde sont construites le long de côtes congestionnées qui sont sur des sols mous et très compressibles jusqu'à des profondeurs importantes. Les dépôts d'argiles marines ou alluviales présentent une faible capacité portante et des tassements importants. Ceci a des implications au niveau du dimensionnement et de la maintenance pour de hautes structures, de grands bâtiments commerciaux ainsi que pour des infrastructures portuaires et de transport construits sur de tels sols de piètre qualité. La stabilisation de ces sols très mous est donc essentielle avant de commencer à construire des infrastructures. Un système de drains verticaux combiné avec du préchargement par le vide et surcharge est devenu une option efficace et économique d'amélioration des sols. Cette technique accélère la consolidation en favorisant un écoulement radial rapide qui réduit les surpressions interstitielles et augmente les contraintes effectives. Cette conférence présente une revue des développements théoriques et pratiques de l'amélioration des sols mous par drains verticaux (incluant ceux en fibres naturelles) et préchargement par le vide, avec application à des cas d'études australiens.

KEYWORDS: PVD, surcharge preloading, vacuum preloading, soft soil, consolidation, NPVD.

1. INTRODUCTION

The booming population and associated development in coastal and metropolitan areas have necessitated the use of previously undeveloped low lying areas for construction purposes (Indraratna et al. 1992; Indraratna 2010). The low bearing capacity and high compressibility of these deposits affect the long term stability of buildings, roads, rail tracks, and other forms of major infrastructure (Johnson 1970). Therefore, it is imperative to stabilise these soils before commencing construction to prevent unacceptable differential settlement. However, attempts to improve deep bearing strata may not be commensurate with the overall cost of the infrastructure (Bo et al. 2003). In the past, various types of vertical drains such as sand drains, sand compaction piles, PVDs (geosynthetic), stone columns, and gravel piles have been used to accelerate consolidation and/or strengthen the soil. PVD are often preferred due to relative low cost and ease of installation. Their installation can significantly reduce the preloading period by decreasing the length of the drainage path, sometimes by a factor of 10 or more. More significantly, PVDs can be rapidly installed with minimal environmental implications and quarrying requirements compared to semi-rigid inclusions.

Preloading, or temporarily loading an area beyond its final loaded state, is one of the most successful techniques for improving the shear strength of low-lying areas (Richart 1957; Indraratna and Redana 2000; Indraratna et al. 2005a). The additional load induces further strength gain in the soil that remains after preload removal. Expected consolidation settlement from the final embankment load is achieved faster with a preload. After preload removal the soil is often in an overconsolidated state which reduces creep related settlement in the post construction period. In order to control embankment stability and reduce the rate of pore pressure build-up, a surcharge embankment is usually raised as a multi-stage exercise, with rest periods between the loading stages (Jamiolkowski et al. 1983). Since most compressible low-lying soils are often thick with very low permeability, a lengthy time period is usually needed to achieve the desired primary degree of consolidation (>95%). In these instances, the height of the surcharge needed to induce rapid consolidation can be excessive from an economic and stability perspective (Indraratna et al. 1994). Long surcharge times may be impractical due to stringent construction schedules. When PVDs combined with surcharge preloading is applied, vertical drains provide a much shorter drainage path in a radial direction which reduces the required preload period significantly. PVDs are cost effective and can be readily installed in moderate to highly compressible soils (up to 40m deep) that are normally consolidated or lightly over-consolidated. PVDs rarely offer particular advantages if installed in heavily over-consolidated clays.

When required consolidation times are very short or the sub-soil is particularly weak, vacuum pressure has been used to enhance the efficiency of PVD. Negative pore pressures (suction) distributed along the drains and on the surface of the ground accelerate consolidation, reduce lateral displacement, and increase the effective stress. This allows the height of the surcharge embankment to be reduced to prevent any instability and lateral movement in the soil. Today, PVDs combined with vacuum preloading are being used more and more in practical ground improvement all over the world. Most of the research

outcomes in this regard can be categorized into 16 themes, as given in Table 1.

This lecture includes salient aspects of more than 20 years of research conducted at the University of Wollongong in the area of soft soil stabilisation using PVDs and vacuum preloading. The research work forms a vital Australian contribution to the field of soft soil improvement as well as offering a significant component of higher education training through more than a dozen doctoral studies to date. The University of Wollongong has and continues to promote the advancement of current industry practices in infrastructure development in coastal and low lying areas.

Table 1. Vertical Drains and Vacuum Consolidation in a Nutsell – Key themes

Theme Description	Selected key References
1. Classical Theories and Fundamentals of Radial Consolidation	Carrillo 1942, Barron 1948, Akagi 1979, Hansbo 1979, 1981, 1997, Onoue 1988, Zeng and Xie 1989, Mohamedelhassan and Shang 2002, Chu et al. 2000, 2014
2. Types of Vertical Drains and Installation Effects	Bo et al. 1998, Saye 2001, Basu and Prezzi 2007, Chai, et al. 2008, Liu and Chu 2009, Basu et al. 2009, 2010, Ghandeharioon et al. 2010, Ong et al. 2012, Indraratna et al. 2015a
3. Smear Zone Analysis and Assessment	Bergado, et al. 1991, Madhav, et al. 1993, Zhu and Yin 2004, Sathananthan and Indraratna 2006, Chung and Lee 2010, Rujikiatkamjorn et al. 2013, Parsa-Pajouh et al. 2014, Choudhary et al. 2016
4. Experimental procedures - from traditional Rowe cells to large Scale testing	Indraratna and Redana 1998, Chai and Miura 1999, Leong, et al. 2000, Sharma and Xiao 2000, Fang and Yin 2006, Saowapakpiboon et al. 2010, 2011, Robinson et al. 2012
5. Mathematical Modelling of Radial Consolidation with and without Vacuum Preloading	Tang and Onitsuka 1997, 2001, Ing and Nie 2002, Leo 2004, Indraratna et al. 2005ab, Basu et al. 2006, Indraratna et al. 2008, Conte and Troncone 2009, Chung et al. 2009, 2014, Walker and Indraratna 2009, Geng et al. 2011, Walker 2011, Walker et al. 2012, Kianfar et al. 2013, Rujikiatkamjorn and Indraratna 2014a, Lu et al. 2015ab, Ho et al. 2014, 2015, 2016, Lei et al. 2015, 2016.
6. Numerical Modelling of Soft Soil embankments stabilized with PVD and VP	Hird et al. 1992, 1995, Indraratna and Redana 1997, Rujikiatkamjorn et al. 2008, Tran and Mitachi 2008, Araújo et al. 2012, Chai et al. 2013, Xu et al. 2015, Lam et al. 2015, Indraratna et al. 2004, 2016a
7. Vacuum consolidation principles	Holtan 1965, Holtz and Wager 1975, Cognon et al. 1994, Gabr and Szabo 1997, Bergado et al. 1998, Chu et al. 2000, Indraratna et al. 2004, 2005ab, Chai et al. 2005, 2008, 2010, Geng et al. 2012, Mesri and Khan 2012
8. Design procedures and Practice Guides (with and without VP)	Asaoka 1978, Holtz et al. 1991, Qian et al. 1992, Chu and Yan 2005ab, Seah 2006, Rujikiatkamjorn and Indraratna 2007, Abuel-Naga et al. 2012, Long et al. 2013, Bari and Shahin 2014, et al.
9. Natural PVD, Biodegradation effects and implications on consolidation	Lee et al. 1987, 1994, Miura et al. 1995, Kim and Cho 2009, Jiang et al. 2001, Kim et al. 2011, Asha et al. 2012, Saha et al. 2012, Deng et al. 2013, Nguyen and Indraratna 2016, Indraratna et al. 2016b
10. Case Studies (Instrumented and Monitored)	Holtan 1965, Choa 1990, Indraratna et al. 1992, Jacob et al. 1994, Shang et al. 1998, Bergado et al. 1998, 2002, Wijeyakulasuriya et al. 1999, Tang and Shang 2000, Yan and Chu 2003, 2005, Shen et al. 2005, Chai et al. 2006, 2013, Indraratna et al. 2005c, 2011, 2012, 2014, Mesri and Khan 2012, Cascone and Biondi 2013, Mesri and Funk 2014, Voottipruex et al. 2014
11. Class A Predictions	Indraratna et al. 1992, 2010, Bergado et al. 1993, Wu et al. 2007
12. Application of PVDs under Cyclic loading	Indraratna et al. 2009, 2015b, Ni et al. 2013, Razouki 2016
13. Large strain analysis of radial consolidation	Fox et al. 2003, Xie and Leo 2004, Venda Oliveira and Lemos 2011, Hu et al. 2014, Indraratna et al. 2016c
14. Creep effects and Visco-plasticity in PVD stabilised soil	Bjerrum 1967 , Yin and Graham 1988, Yin and Clark 1994, Mesri et al. 1987, 1997, Yun and Leroueil 2001, Nash and Ryde 2001, Indraratna et al. 2007, Azari et al. 2016, et al.
15. Implications of Clogging, Kinking and Bending of PVD	Lawrence and Koerner 1988, Holtz et al. 1989, Bergado et al. 1996, Basu and Madhav 2000, Aboshi et al. 2001
16. Miscellaneous Topics	Lee and Xie 1996, Wang and Jiao 2004, Chen et al. 2005, Brennan and Madabhushi 2006, Yildiz et al. 2009, Marinucci et al. 2008, Marinucci 2010, Mirjalili et al. 2012, Ye et al. 2012, Howell et al. 2012, Zhou and Zhao 2013, Zhou 2013, Liu et al. 2014, Rujikiatkamjorn and Indraratna 2014b, Karim and Lo 2015, Ho and Fatahi 2016

2. THEORETICAL DEVELOPMENTS OF PVD AND VACUUM CONSOLIDATION

The vacuum preloading method for vertical drains was arguably first introduced by Kjellman (1952) in Sweden. Since then, it has been used extensively to accelerate the consolidation of soft ground worldwide, for instance at the Philadelphia International Airport, USA; Tianjin port, China; North South Expressway, Malaysia; Reclamation works in Singapore and Hong Kong, China; Suvarnabhumi Second Bangkok International Airport, Thailand; Ballina Bypass New South Wales and the Port of Brisbane, Queensland in Australia, among many other projects (Holtan 1965; Choa 1990; Jacob et al. 1994; Bergado et al. 2002; Chu et al. 2000; Yan and Chu 2003). To obtain sufficent strength gain and limit post construction settlement in a reasonable time frame, traditional surcharge-only embankments can become excessively high. In a combined vacuum and fill surcharge approach the vacuum can provide the surcharge removing the need for additional fill.

In very soft clays where a high surcharge embankment cannot be constructed without affecting stability (large lateral movement) or having to work within a tight construction schedule, the application of vacuum pressure is quite often the most appropriate choice. The theoretical maximum suction attainable is atmospheric pressure of approximately 100 kPa. PVD-vacuum systems are designed to distribute the vacuum (suction) pressure to deep layers of the subsoil to increase the consolidation rate of reclaimed land and deep estuarine plains (e.g. Indraratna et al. 2005b; Chu et al. 2000). This section touches on drain and soil properties relevant for modelling consolidation processes in PVD and vacuum systems.

2 .1 *Vacuum consolidation theory capturing smear effect*

Mohamedelhassan and Shang (2002) developed a combined vacuum and surcharge load system based on Terzaghi one-dimensional consolidation theory (Figure 1). The mechanism for the combined vacuum and surcharge loading (Figure 1a) may be determined by the law of superposition (Figure 1b and Figure 1c). The average degree of consolidation for combined vacuum and surcharge preloading can then be expressed by:

$$U_{vc} = 1 - \sum_{m=0}^{\infty} \frac{2}{M} \exp^{-M^2 T_{vc}} \tag{1}$$

$$T_{vc} = c_{vc} t / H^2 \tag{2}$$

where T_{vc} is a time factor for combined vacuum and surcharge preloading, and c_{vc} is the coefficient of consolidation for combined vacuum and surcharge preloading.

Indraratna et al. (2004) showed that when vacuum pressure is applied in the field through PVDs, the suction head along the length of the drain may decrease with depth, thereby reducing its efficiency. Laboratory measurements taken at a few points along PVDs installed in a large-scale consolidometer at the University of Wollongong clearly indicated that the vacuum propagates immediately, but a gradual reduction in suction may occur along the length of the drain. The distribution of suction in a PVD depends mainly on the length and type of PVD (core and filter properties). However, some field studies suggest that the suction may develop rapidly even if the PVDs are up to 30 m long in properly implemented vacuum system (Bo et al. 2003; Indraratna et al. 2005a).

Indraratna et al. (2004, 2005a) proposed a modified radial consolidation theory inspired by laboratory observations to include different distribution patterns of vacuum pressure (Figure 2). These results indicated that the efficiency of the PVD depended on the magnitude and distribution of the vacuum. In order to quantify the loss of vacuum, a trapezoidal distribution of vacuum pressure along the length of the PVD was assumed.

Based on these assumptions, the average excess pore pressure ratio ($R_u = \Delta p / \bar{u}_0$) of a soil cylinder for radial drainage that incorporates vacuum preloading can be given by:

$$R_u = \left(1 + \frac{p_0}{\bar{u}_o}\frac{(1+k_1)}{2}\right)\exp\left(-\frac{8T_h}{\mu}\right) - \frac{p_0}{\bar{u}_0}\frac{(1+k_1)}{2} \tag{3}$$

and

$$\mu = \ln\left(\frac{n}{s}\right) + \left(\frac{k_h}{k_s}\right)\ln(s) - 0.75 + \pi z(2l - z)\frac{k_h}{q_w}\left\{1 - \frac{k_h/k_s - 1}{(k_h/k_s)(n/s)^2}\right\} \tag{4}$$

where p_0 = vacuum applied at the top of the drain, k_1 = ratio between the vacuum at the top and bottom of the drain, u_0= initial excess pore water pressure, k_h, k_s = horizontal permeability in undisturbed and smeared zones, T_h = time factor, $n = d_e/d_w$ (d_e is the diameter of the equivalent soil cylinder = $2r_e$ and d_w is the diameter of the drain = $2r_w$), $s = d_s/d_w$ (d_s is the diameter of the smear zone = $2r_s$ with constant permeability), z = depth, l = equivalent length of drain, q_w = drain discharge capacity.

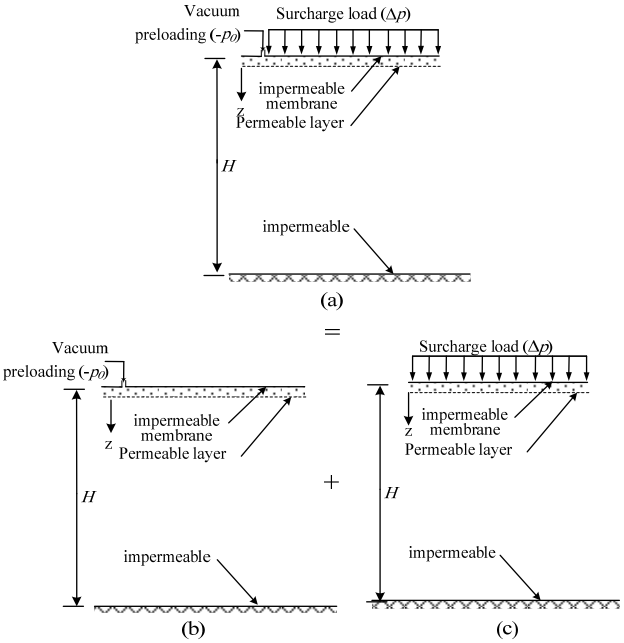

Figure 1. Schematic diagram of vacuum preloading system: (a) combined vacuum and surcharge; (b) surcharge only; and (c) vacuum only(after Mohamedelhassan and Shang 2002, with permission from NRC Research Press).

2 .2 *Analytical modelling of overlapping smear zones*

Installing vertical drains with a steel mandrel significantly remoulds the subsoil in the vicinity of the drain. The smeared zone has reduced lateral permeability and increased compressibility. In varved clays, the finer and more impervious layers are dragged down and smeared over the more pervious layers which in turn decrease the permeability of the soil near the periphery of the drain. Barron (1948) suggested the concept of reduced permeability by arbitrarily lowering the apparent value of the coefficient of consolidation. Hansbo (1981)

modelled a smear zone of constant reduced permeability around a vertical drain. The resulting expression for the smear zone permeability/geometry parameter μ (Eq. (4)), is commonly used in design despite laboratory evidence showing that the reduction of permeability towards the drain is gradual. Despite numerous analytical solutions (many of them involving the author) for variable smear zone permeability distributions the simple expression is preferred due to the difficulty of assessing actual insitu smear zone properties. The success of such an approach is due to the fact that all the various smear zone permeability distributions produce a numerical value of μ. Thus a suitably sized constant permeability smear zone will produce the same μ value as a more realisticic parabolic distribution. In back calcuating consolidation properties from field results it is μ that is back calcuated, and the size and shape of the smear zone are simply assumed.

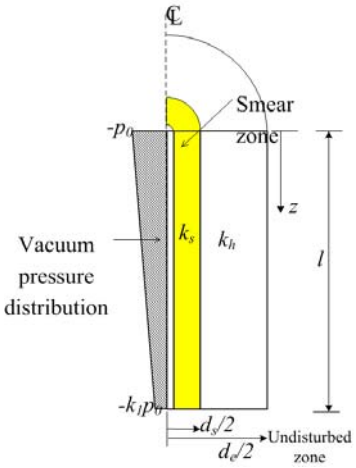

Figure 2. Vertical distribution of vacuum pressure within a PVD (after Indraratna et al. 2005a, with permission from NRC Research Press).

Assuming a constant permeability smear zone will give a small smear zone when compared to one with gradual change. This in turn means there is little chance of these smaller smear zones overlapping. Walker and Indraratna (2007) investigated the possibility of overlapping smear zones with linear permeability distributions. The μ expressions for a single non overlapping linear smear zone are, for $s \neq \kappa$ and $s = \kappa$, respectively:

$$\mu_L = \ln\left(\frac{n}{s}\right) - \frac{3}{4} + \frac{\kappa(s-1)}{s-\kappa}\ln\left(\frac{s}{\kappa}\right) \quad (5)$$

$$\mu_L = \ln\left(\frac{n}{s}\right) - \frac{3}{4} + s - 1 \quad (6)$$

As illustrated in Figure 3, two smear zones will interact when the spacing parameter n is less than the size parameter s of the smear zone. As an idealization, it is assumed the interaction exhibits radial symmetry. It is also assumed that in the 'interaction zone' the permeability is constant at a value of k_X, which is the value of permeability where the smear zones begin to overlap, s_X. So the problem is now addressed by a modified version of the original linearly varying equations. The modified permeability ratio, $\kappa_X = k_X / k_0$ is given by:

$$\kappa_X = 1 + \frac{\kappa - 1}{s-1}(s_X - 1) \quad (7)$$

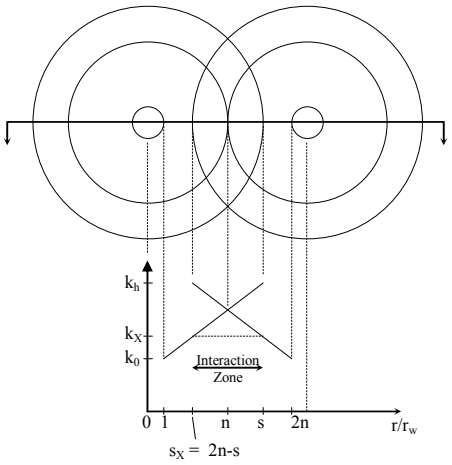

Figure 3. Schematic of overlapping smear zones (Walker and Indraratna 2007, with permission from Thomas/Telford Ltd.)

For the case when $2n - s > 1$, the two smear zones completely overlap; it is then assumed that the permeability is constant at values equal to that at the drain/soil interface (i.e k_0. With reference to the undisturbed values of soil properties a new modified expression, μ_X, describing the effect of interacting smear zones can be defined as:

$$\mu_X = \begin{cases} \mu_L[n, s, \kappa] & n \geq s \\ \dfrac{\kappa}{\kappa_X}\mu_L[n, s_X, \kappa_X] & 2n - s \geq 1, \text{ and, } s > n \\ \dfrac{\kappa}{\kappa_X}\mu_I[n] & 2n - s < 1 \end{cases} \quad (8)$$

Figure 4 shows the time to reach 90% consolidation for a case of overlapping smear zones. It suggests that if not for an absolute drain spacing minimum, there at least exists a range of drain spacing values across which the time required to reach a certain degree of consolidation does not change. For drain spacing values less than the corresponding local minima, the time for consolidation decreases rapidly. This is due to the assumption that once the linear smear zones completely overlap there is no further change in the soil properties; that is, a threshold level of disturbance is reached. This assumption is questionable as at an increasingly closer drain spacing the soil may become further remoulded, exhibiting properties different to that of the partially remoulded smear zone.

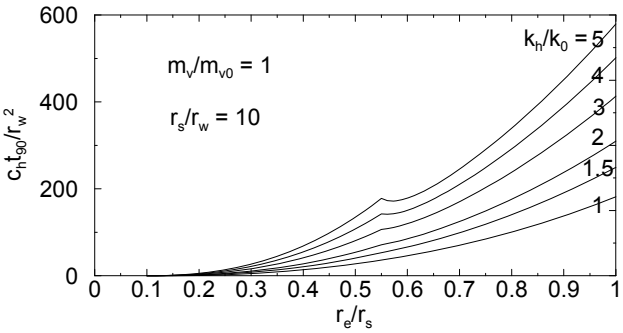

Figure 4. 90% consolidation times with overlapping smear zones (Walker and Indraratna 2007, with permission from Thomas/Telford Ltd.)

2 .3 *Effect of transition zone surrounding smear zone*

Madhav et al. (1993) proposed that the zone disturbed by mandrel driving can be divided into two zones, which are: (i) the smear zone immediately surrounding the PVD and (ii) the transition zone surrounding the smear zone (Figure 5). Basu et al. (2010) studied the effect of transition zone and smear zone on the rate of consolidation with a 2D finite element analysis. Instead of the equivalent circular drain and influence area, actual band shape of PVD and rectangular shape of the influential zone were considered in that analysis.

The numerical analysis was validated by comparison with the experimental data of Indraratna and Redana (1998), in which the outer diameter of the smear and transition zones were approximately $2d_m$ and $7d_m$, respectively. The settlement history was obtained with and without considering the transition zone, and the results were plotted in Figure 6. Also plotted in Figure 6 are the test data of the settlement measured by Indraratna and Redana (1998). The results with expanded smear zone agreed reasonably well with the measured data. When the transition zone was ignored, a significant disagreement to the test measurement was observed in the prediction in the latter part of consolidation.

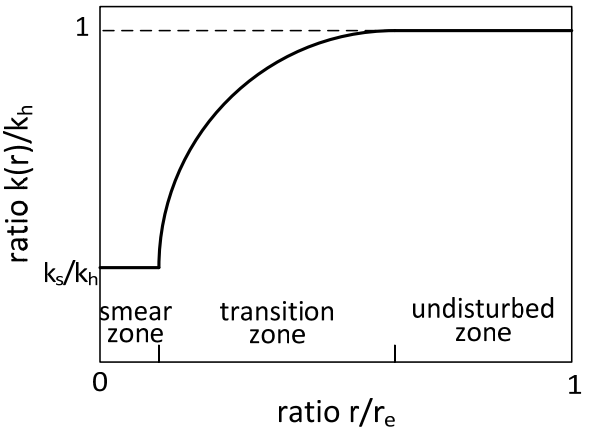

Figure 5. Variation of permeability with distance from centre of mandrel (modified after Madhav et al. 1993).

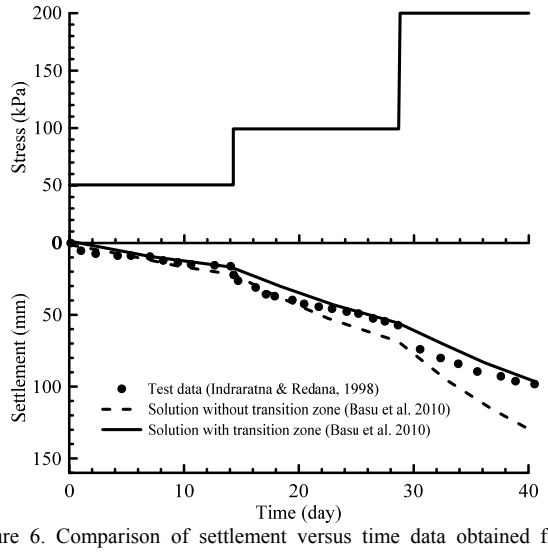

Figure 6. Comparison of settlement versus time data obtained from analysis capturing transition zone with the experimental data of Indraratna and Redana (1998) (modified after Basu et al. 2010).

2 .4 *Non-linear soil properties and soil structure characteristics*

Although mathematically convenient to work with linear governing equations for vertical drain consolidation, the non-linear properties of the soils should be used when modelling realistic soil behaviour. The non-linear variation of soil permeability and compressibility with the void ratio was incorporated into the equal-strain governing equation for vertical drain consolidation by Indraratna et al (2005d). The non-linear relations between the void ratio e and the soil properties (permeability and compressibility) are:

$$e = e_0 + C_k \log\left(\frac{k}{k_0}\right) \tag{9a}$$

$$e = e_0 - C_c \log\left(\frac{\sigma'}{\sigma'_0}\right) \tag{9b}$$

where k_0 and σ'_0 are the soil permeability and vertical effective stress corresponding to e_0.

Besides the non-linear permeability and compressibility of the soil, exponential non-Darcian flow and pre/post yield behavior was considered by Walker et al. (2012). The governing equation with the average excess pore pressure $\bar{u}$ as the unknown was obtained as:

$$\bar{u} = \left(\gamma_w r_w\right)^{1-1/n} \beta \left(-\frac{r_e^2}{2\tilde{c}_h}\frac{\partial \bar{u}}{\partial t}\right)^{1/n} \tag{10}$$

where $\bar{u}$ is the average excess pore pressure, n is the non-Darcian flow exponent, and $\tilde{c}_h$ is the coefficient of consolidation, and β is the non-Darcian radial consolidation parameter defined by Walker et al. (2012).

A laboratory test using the large-scale consolidometer (with a height of 950 mm and a diameter of 450 mm) at the University of Wollongong was carried out with reconstituted alluvial clay from Moruya, NSW in Australia. The value of C_c and C_k were tested to be 0.29 and 0.45, respectively. Results of the two tests with different preconsolidation pressure and load were compared against the predictions of Indraratna et al. (2005d) and Walker et al. (2012), as shown in Figure 7. The comparison indicated that the analytical solutions agree well with the test data, and the result using the Walker et al. (2012) formulation agrees slightly better with the test data than that of Indraratna et al. (2005d).

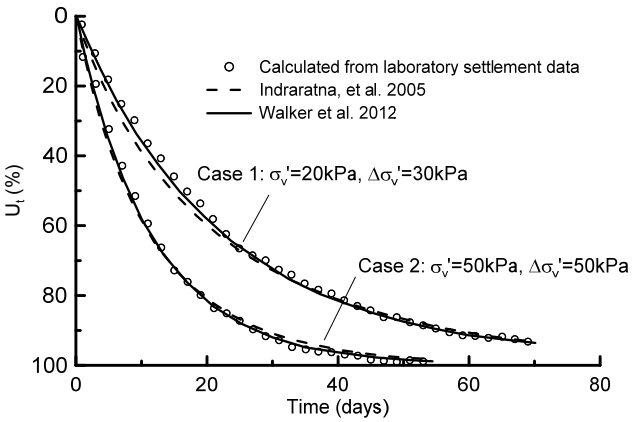

Figure 7. Comparison between test data and predictions (Walker et al. 2012, with permission from Thomas Telford Ltd.).

The ratio of C_d/C_k also has a significant effect on consolidation rate. For $C_d/C_k < 1$ consolidation was faster than the conventional linear solution; while for $C_d/C_k > 1$ consolidation was slower than the linear solution.

Although Eq. (9b) is more realistic than the linear relation adopted in the conventional approaches, it is only valid for reconstituted soils. The *in situ* behaviour of soft clays could be very different from the laboratorial investigations, which is why Rujikiatkamjorn and Indraratna (2014a) developed an analytical solution for radial consolidation that considers the soil structure characteristics by incorporating variable void ratio-effective stress relationship. The conceptual model for soils disturbed by mandrel action (Rujikiatkamjorn et al. 2013) was used, as shown in Figure 8.

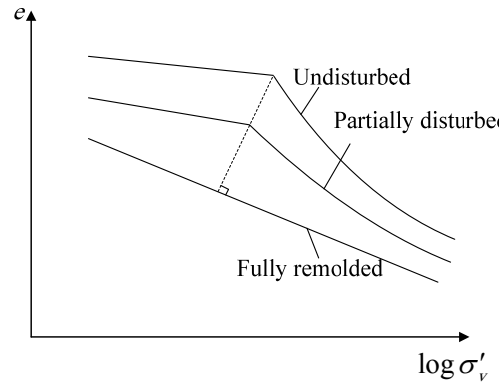

Figure 8. Conceptual compression behaviour of soil with different disturbance levels (modified from Rujikiatkamjorn et al. 2013, 2014a, with permission from NRC Research Press).

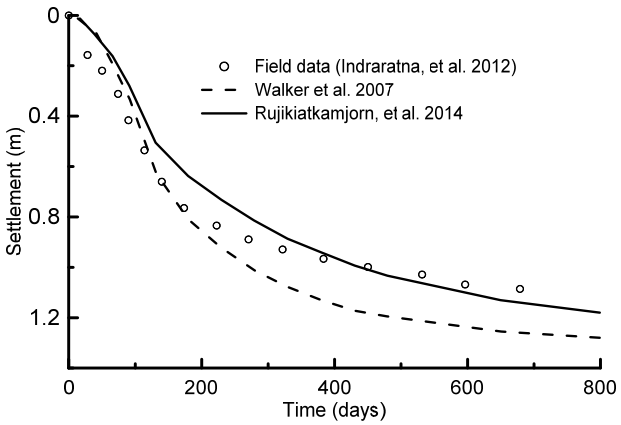

Figure 9. Predicted and measured settlement in SP1 at Ballina Bypass (adapted from Rujikiatkamjorn and Indraratna, 2014a, with permission from NRC Research Press).

Figure 9 shows a comparison of settlement plots for the Ballina Bypass project based on two analytical solutions proposed by Walker and Indraratna (2007) and Rujikiatkamjorn, et al. (2014a). Walker and Indraratna (2007) captured the linear variation of permeability in the smear zone, whilst Rujikiatkamjorn and Indraratna (2014a) considered the effects of soil disturbance on both permeability and compressibility in the smear zone. The results indicated that the method capturing the effect of soil disturbance on both permeability and compressibility can result in a better match with the field data, and shows the importance of mandrel induced soil structure degradation.

2.5 *Large strain effect*

Soft estuarine deposits may experience large strains when consolidated via PVD under extensive surcharge and vacuum preloading. Indraratna et al. (2016c) proposed a large strain consolidation model incorporating varying permeability and compressibility, non-Darcian flow as well as large strain effect for PVD consolidation. Under low hydraulic gradients in low porosity soils fluid flow may deviate from Darcy's law. The Non-Darcy behavior is typically considered as an exponential relationship between the seepage velocity and the hydraulic gradient.

Based on a large strain coordinate system, the Lagrangian coordinate a and the convective coordinate ξ have the relationship $\frac{\partial \xi}{\partial a} = \frac{1+e}{1+e_0}$ where e is the void ratio and e_0 is the initial void ratio. A large-strain governing equation with radial flow has been established as:

$$\frac{1}{1+e_i} \cdot \frac{\partial e}{\partial t} \cdot \mathrm{d}a + v_r(r) \cdot \frac{2r}{r_e^2 - r^2} \cdot \frac{\partial \xi}{\partial a} \mathrm{d}a = 0 \qquad (11)$$

where r is the radius, r_e is the drain influence radius, t is the time, and $v_r(r)$ is the inward seepage velocity at radius r.

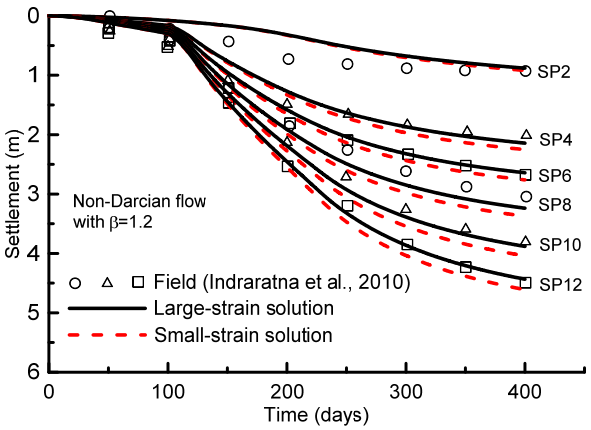

Figure 10. Comparison between large-strain and small-strain solution at Ballina Bypass. (Indraratna et al. 2016c, with permission from ASCE)

Numerically solving Eq.(11), Figure 10 compares settlement predictions from small and large-strain analyses with field data from a Ballina Bypass embankment. Figure 10Having compared the large-strain with the small-strain settlement results, Figure 10 clearly indicates that the proposed large-strain solution gives a more acceptable prediction of settlement at each settlement plate location.

2.6 *Degree of consolidation theory based on pore pressure*

Assessement of degree of consolidation in the field is normally based on either monitored ground settlement or excess pore water presure. Chu and Yan (2005b) proposed a method to estimate the average degree of consolidation based on pore water pressure. This method requires the measurement of pore water pressures at various depths, and the plot of the initial and final pore water pressure distributions is schematically illustrated in Figure 11. The average degree of consolidation can then be determined by:

$$U_{avg} = 1 - \frac{\int [u_t(z) - u_s(z)]\,dz}{\int [u_0(z) - u_s(z)]\,dz} \quad (12)$$

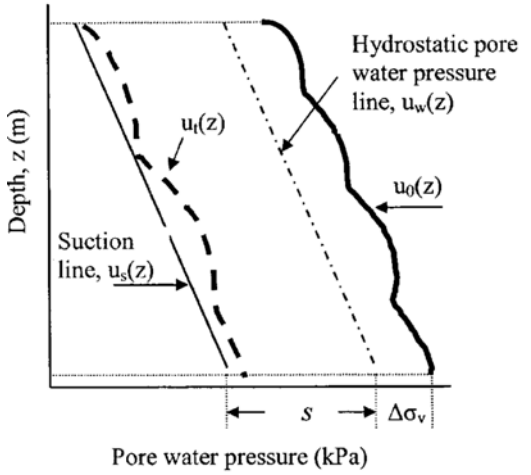

Figure 11. Illustration of pore water distribution with depth (Chu and Yan 2005b, with permission from ASCE).

This method has multiple advantages compared to the method of estimating degree of consolidation based on ground settlement, such as:

(1) Pore pressure data required by this method are all directly measured; whereas the method based on ground settlement requires a predicted ultimate settlement;

(2) It can calculate not only the final degree of consolidation, but also that at any time;

(3) For multiple layers, the method can be applied to each layer individually.

2 .7 *Lateral deformation theory*

Chai et al. (2013) proposed an empirical equation for estimating the lateral displacement of ground improved with PVDs subjected to fill surcharge and vacuum preloading. A dimensionless parameter, i.e. the normalized maximum value of net lateral displacement (NLD), was proposed and expressed as

$$\text{NLD} = \frac{\delta_{mo} - |\delta_{mi}|}{S_f} \quad (13)$$

where δ_{mo} and δ_{mi} are the maximum values of the net outward lateral displacement and inward lateral displacement, respectively, S_f is the settlement of the ground at the centerline of the embankment.

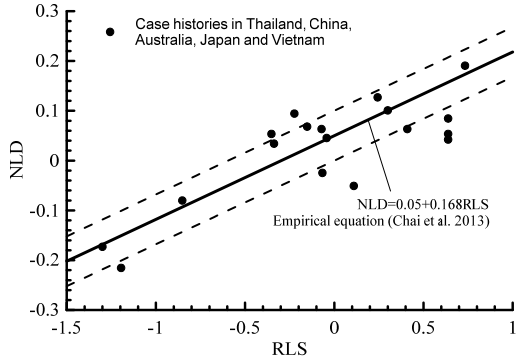

Figure 12. Ratio of index pressure to representative shear strength–normalised maximum (net) lateral displacement (RLS–NLD) relationship (modified from Chai et al. 2013, with permission from Thomas Telford Ltd.)

Another dimensionless parameter, the representative shear strength (RLS), was expressed as:

$$\text{RLS} = \frac{p_{em} - (|p_{vac}| + p_{em})U}{s_u} \quad (14)$$

where p_{em} and p_{vac} are the embankment pressure and the vacuum pressure, respectively, U is the average degree of consolidation of the treated area at the end of the embankment construction period, and s_u is the representative undrained shear strength of the subsoil.

Eighteen case histories from Thailand, China, Australia, Japan and Vietnam were studied to investigate the relationship between RLS and NLD (Figure 12). A general relationship was proposed as NLD=0.05+0.168RLS (for -1.5<RLS<0.75). This method may be used to estimate the likely range of the NLD, in designing ground improvement works in soft clay using the PVDs under a combination of vacuum pressure and embankment pressure.

3. EXPERIMENTAL SIMULATIONS

Trial field embankments and laboratory consolidometer tests (cylinders of soil with a central drain) have been used to verify/quantify many of the theoretical effects discussed in the previous section. In particular, the University of Wollongong's large scale consolidometers have been used extensively to study the smear zone around a PVD. This section describes a range of experiments including recent tests with cyclic loading.

3.1 *Large scale testing of smear zone*

Based on constant but reduced permeability in the smear zone, Jamiolkowski et al. (1983) proposed that the diameter of the smear zone (d_s) and the cross section of the mandrel can be related by:

$$d_s = (2.5 \text{ to } 3)\, d_m \quad (15)$$

In the above, d_m is the diameter of the circle with an area equal to the cross section of the mandrel (i.e. equivalent mandrel diameter). Based on the results of Akagi (1979) and Hansbo (1987), the smear zone is often evaluated by the simple expression:

$$d_s = 2\, d_m \quad (16)$$

Onoue et al. (1988) introduced a three zone hypothesis defined by (a) a plastic smear zone close to the drain where the soil is highly remoulded during installation, (b) a plastic zone where the permeability is reduced moderately, and (c) an outer undisturbed zone where the soil is unaffected by installation.

On the basis of their experimental work, Indraratna and Redana (1998) proposed that the estimated smear zone is at least 3-4 times larger than the cross section of the drain. This proposed relationship was verified using a specially designed large scale consolidometer (the schematic section is shown in Figure 13). Figure 14 shows the variation of the ratio of horizontal to vertical permeability (k_h/k_v), and the water content along a radial distance from the central drain in the large scale consolidation apparatus (Indraratna and Redana 1998; Sathananthan and Indraratna 2006; Walker and Indraratna 2006). The radius of the smear zone is about 2.5 times the equivalent radius of the mandrel. The lateral permeability (within the smear zone) is 61%~92% of the outer undisturbed

zone, which is similar to Hansbo (1987) and Bergado et al. (1991) recommendations. Only recently, Sathananthan et al. (2008) used the cavity expansion theory (CET), with the modified Cam-clay model, to analyse the extent of the smear zone caused by mandrel driven vertical drains. Their predictions were verified by large scale laboratory tests where the extent of the smear zone was quantified based on (a) response of excess pore pressure generated while driving the steel mandrel, (b) change in lateral permeability, and (c) reduction in soil water content towards the drain.

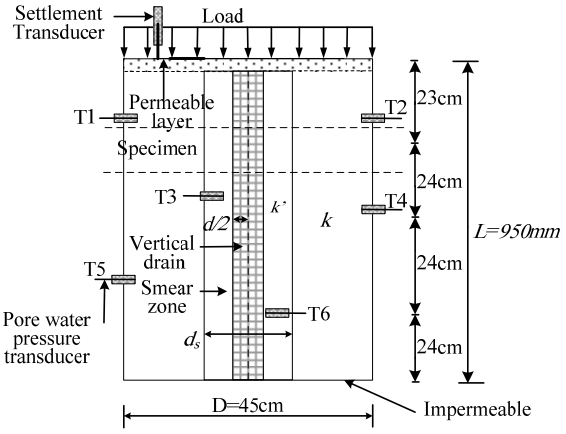

Figure 13. Schematic section of the test equipment showing the central drain and associated smear (Indraratna and Redana 1998, with permission from ASCE).

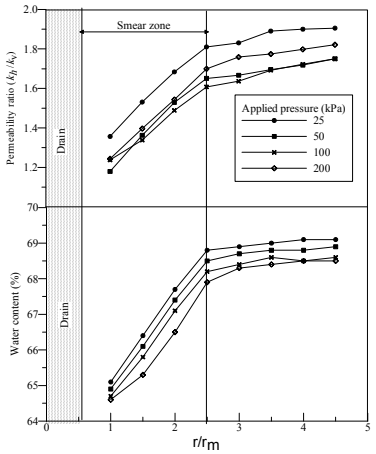

Figure 14. Smear zone determination using: (a) permeability ratio; and (b) water content (Sathananthan and Indraratna 2006, with permission from ASCE).

3.2 *Full-scale embankment test investigating smear zone*

A full-scale field embankment test was analysed by Bergado et al. (1991) to investigate the effect of smear effect by mandrel driving on an area 15 m × 19 m. A total of 168 band drains with cross-sectional dimensions of 100 mm × 6 mm were driven to a depth of 8 m in a square pattern with 1.2 m drain-to-drain spacing using two different sizes of mandrels: 150 mm × 45 mm and 150 mm × 150 mm (see Figure 15).

Figure 16 shows that the dissipation of pore pressures in the large mandrel region is slower than that in the small mandrel region. Extensometer settlement data show that the small mandrel region has a considerably faster settlement rate than the large mandrel region (Figure 17), probably because a smaller smear zone has been caused by the smaller mandrel. This test indicates that the smear effect is closely related to the size of the mandrel and plays an important role in the effectiveness of ground improvement using vertical drains.

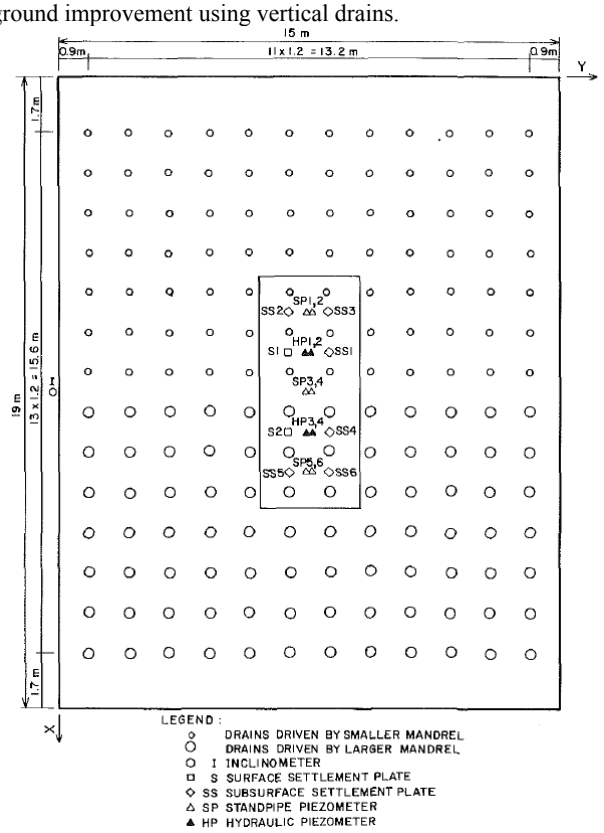

Figure 15. Layout of vertical drains in the full-scale embankment test (Bergado et al. 1991, with permission from ASCE).

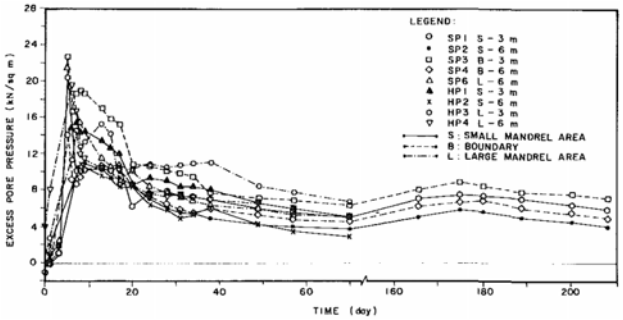

Figure 16. Measured pore pressure of the full-scale embankment test (Bergado et al. 1991, with permission from ASCE).

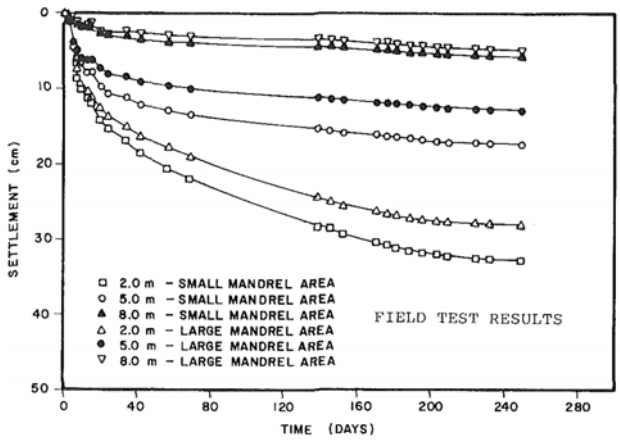

Figure 17. Measured settlement of the full-scale embankment test (Bergado et al. 1991, with permission from ASCE).

3.3 *Pore pressure based method to quantify smear for vertical drains*

A set of large consolidometer cells (see Figure 13) was set up at the University of Wollongong to investigate smear characteristics of jute drains made from coconut fibres (Choudhary et al. 2016). Seven pore pressure transducers were placed 100 mm from the bottom of the cell in a staggered arrangement around the drain (i.e. 15, 30, 45, 60, 100, 150, 200 mm from the centreline) to measure the pore pressure in the soil-drain system at different radii. Sample height, moisture content and permeability were measured both prior to and after the consolidation test. Soil was extracted from a flood plain from a depth of 2m from Ballina Bypass whose properties have been described in detail in Indraratna et al. 2015a.

The plot for the degree of consolidation is shown in Figure. 18 and is compared with the theoretical calculations of consolidation considering a linear and a parabolic variation of permeability in the smear zone. The degree of consolidation (U_t) was derived from the equation suggested by Carrillo (1942), hence,

$$U_t = 1 - \sum_{m=1}^{\infty} \frac{8}{(2m+1)^2 \pi^2} \exp\left(-\left[\left(\frac{2m+1}{2} \right)^2 \pi^2 \frac{k_v t}{m_v \gamma_w l^2} + \frac{8}{\mu} \frac{k_h t}{m_v \gamma_w d_e^2} \right] \right) \quad (17)$$

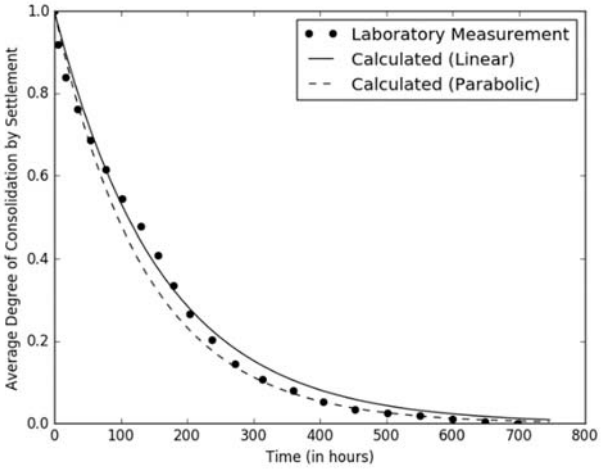

Figure. 18 Time-Settlement curve of jute drain-soil system and its comparison with theoretical calculations based on linear and parabolic permeability profiles in the Smear Zone. (Choudhary et. al. 2016, with permission from Thomas Telford Ltd.)

The theoretical calculations based on the variations in permeability are found to be in acceptable agreement with the measured data. The experimental data obtained from our system agrees with the parabolic case for later part of the consolidation process and with the linear case for the initial consolidation process. The variation of permeability in the smear zone thus plays an important role in determining the correct consolidation response. The pore water pressure variation with radius was used to develop a new method of determination of smear zone (Choudhary et. al., 2016). The variations of normalized permeability (k_h/k_v) and normalized moisture content (w_{max}-w/w_{max}) have been presented in Figure. 19 and compared with Sathananthan and Indraratna (2006). r and r_m denote the distance from the centreline and the effective radius of the mandrel respectively. It can be observed that the normalized permeability increases from a value of 1.6 at r = 15 mm to a value of 2.2 at r = 100 mm and remains constant thereafter thus demarcating the extent of the smear zone. A similar trend is also found in the plot for normalized water content indicating the radius of the smear zone to be nearly 100 mm. This is found to be in agreement with the values provided by Sathananthan and Indraratna (2006).

The distribution of excess pore pressure within the unit cell was also examined. Based on equation (17) for a given depth z and a time t, the radial derivative of excess pore pressure, i.e. du/dr is plotted in Figure 19(c) for cases with and without smear, the latter being the theoretical plot based on Barron (1948), while the former is plotted using the experimental data. Observing that (a) the variation of k_h' along the radial direction would converge to the constant horizontal permeability in the undisturbed zone and (b) du/dr is inversely proportional to the horizontal permeability when the vertical permeability is constant in the unit cell, the plots of du/dr for both cases (i.e. 'with smear' and 'without smear') can be used to determine the extent of smear zone based on the intersection of these two curves. Based on the proposed method, Figure 19(c) gives the smear zone size to be close to r/r_m =2·5.

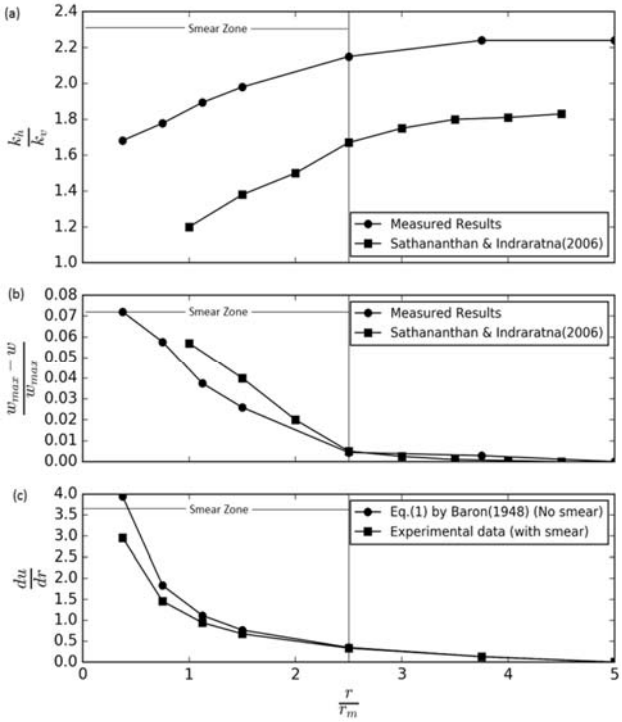

Figure. 19 Variation of permeability and normalized water content from the centreline (Choudhary et. al. 2016, with permission from Thomas Telford Ltd.)

3.4 *Large scale consolidometer test under vacuum consolidation*

Saowapakpiboon et al. (2010) conducted a series of laboratory tests using a large scale consolidometer with an inner diameter of 305 mm and a height of 500 mm. Soft clay samples were obtained from 3 to 4 m depth at the sites of the Second Bangkok International Airport and the Suvarnabhumi Airport in Thailand. The specimens were prepared with the reconstituted soils under a preconsolidation pressure of 50 kPa.

One specimen was consolidated with PVD under a vertical stress of 100 kPa, while the other specimen was used a combination of 50 kPa vertical stress and -50 kPa vacuum pressure. The pressures were applied and vertical displacement was measured immediately after PVD installation. The final

settlements between the specimen with vacuum preloading and the specimen without vacuum preloading were compared and are given in Figure 20. The settlement rate of the surcharge+vacuum case was considerably faster than that of the surcharge-only case.

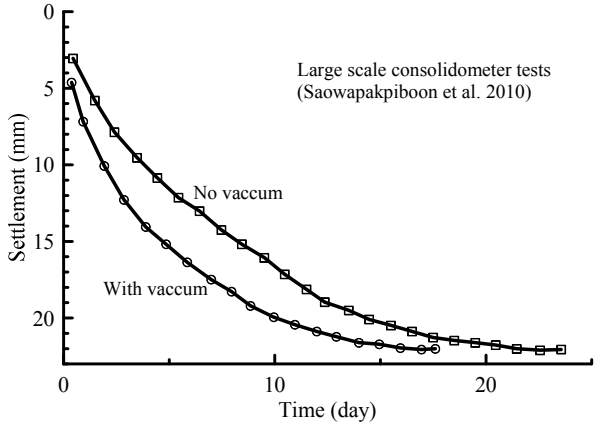

Figure 20. Settlement history from large consolidometer of reconstituted sample in the laboratory using PVDs with and without vaccum (adopted from Saowapakpiboon et al. 2010, with permission from Elsevier).

3.5 *Large scale testing of PVD subjected to cyclic loading*

Plastic clays can exhibit high excess pore water pressure during static and repeated loading. The effectiveness of PVDs for dissipating cyclic pore water pressures has been discussed by Indraratna et al. (2009). This research was particularly beneficial for fast freight trains travelling on trucks constructed on soft soil terrains along the coast, and where 'mud pumping' is a potential problem.

A large scale triaxial test was used to examine the effects of cyclic load on radial drainage and consolidation by PVDs (Figure 21a). This test chamber can accommodate specimens 300 mm diameter and 600 mm high (Figure 21b). The excess pore water pressure was monitored via miniature pore pressure transducers fitted through the base of the cell to the desired locations on the samples.

(a) (b)

Figure 21 (a) Large-scale tri-axial rig; (b) soil specimen (Indraratna et al. 2009, with permission from ASCE).

The test specimen of reconstituted estuarine clay was lightly compacted to a unit weight of about 17 to 17.5 kN/m^3. Ideally, testing requires the simulation of k_0 conditions that in many coastal regions of Australia typically vary from 0.6-0.7. Most soft clays will have natural water contents that exceed 75% and a Plasticity Index > 35%. It is not uncommon to find that the undrained shear strengths of the soft estuarine deposits are less than 10 kPa. In Northern Queensland, some very soft clays that have caused embankment problems have been characterised by c_u values < 5 kPa.

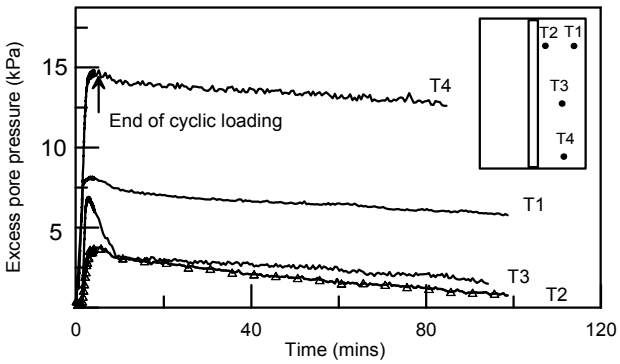

Figure 22. Dissipation of excess pore pressure at various locations from the PVD (Indraratna et al. 2009, with permission from ASCE).

The tests were conducted at frequencies of 5-10 Hz and under cyclic load amplitude of 25 kPa, simulating train speeds of 60-100 km/h with 25-30 tonnes/axle loads. Figure 22 shows an example of the excess pore pressure recorded at various locations within the cell. The maximum excess pore water pressure closer to the PVD (T2) during cyclic load was significantly less than that near the cell boundary (T1), and the dissipation rate of excess pore pressure at T2 (close to the PVD) was faster than that of T1.

The excess pore water pressure ratio R_u is defined as the ratio between the excess pore pressure and the initial effective pressure (Miller et al. 2000; Zhou and Gong 2001). Figure 23 shows the excess pore pressures and corresponding excess pore water pressure ratio R_u versus the number of loading cycles N under the three separate series of tests. Without PVD, the excess pore pressure increased rapidly $R_u \approx 0.9$, and undrained failure occurred very quickly. The corresponding axial strains are shown in Figure 24a. Without a PVD, large cyclic axial strains developed and failure occurred rapidly after about 200 cycles in the cyclic CK_0U test, and after about 100 cycles in the cyclic UC (cyclic confined compression) test. Figure 24b indicates failure initiation when the $\varepsilon_a - \log N$ curves become concave downwards. With a PVD, the axial strain gradually increased to a constant level and no failure was evident even after 3,000 cycles, as shown in Figure 24 (a&b).

The test results revealed that PVDs decreased the maximum excess pore pressure under cyclic loading. They also decreased the build-up of excess pore pressure and helped to accelerate its dissipation during any rest periods. In reality, dissipating pore water pressure during a rest period stabilises the track for the next loading stage (i.e. subsequent passage of train). This cyclic-induced excess pore pressure tends to rise substantially as the shear strain exceeds 1.5-2%. Soft clays provided with radial drainage via PVD can be subjected to cyclic stress levels higher than the critical cyclic stress ratio without causing undrained failure.

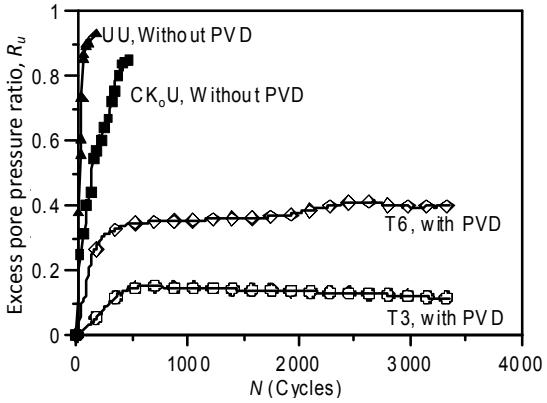

Figure 23. Excess pore pressure generated with and without PVD under cyclic loading (Indraratna et al. 2009, with permission from ASCE).

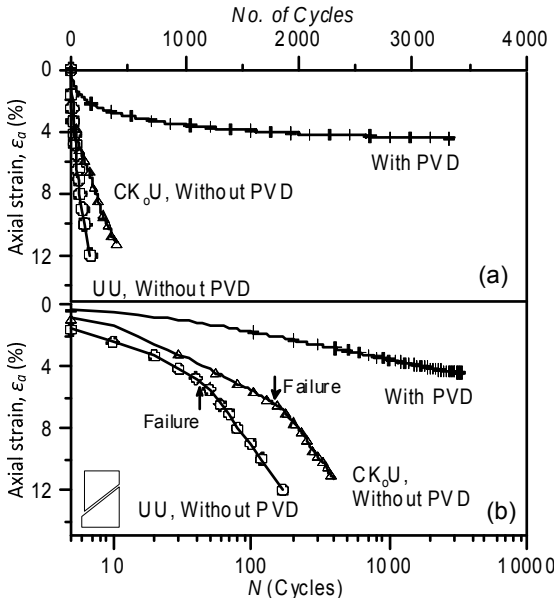

Figure 24. Axial strains during cyclic loading with and without PVD versus number of loading cycles (N): (a) arithmetic; (b) semi logarithmic scales (Indraratna et al. 2009, with permission from ASCE).

4. CONSTITUTIVE MODEL OF SOFT SOILS UNDER CYCLIC LOADING

Conventional application of PVD and vacuum to embankments involves relatively static loads. The previous section suggests PVD can be used in areas with highly oscillatory loads to reduce pore pressure build up and deformations such as those occurring under railway tracks. This relatively new area requires understanding of clay behaviour subject to cyclic loads. A constitutive model for soft soils under cyclic loading was presented by Ni et al. (2015).

Compared to the static behaviour, the cyclic behaviour of soft subgrade soils is more complex as the excess pore pressure and strain continue to develop with increasing number of cycles. Ni et al. (2015) extended the Modified Cam-clay-based cyclic soil model of Carter et al. (1980, 1982) considering the dependence of the excess pore pressure generation rate on the number of cycles. Only two additional parameters are included in the parameters of Modified Cam Clay model. It is assumed that during elastic unloading, the yield surface remains unchanged, but reduces the size in an isotropic manner (Carter et al. 1980, 1982) as follows:

$$\frac{\mathrm{d}p_{\mathrm{c}}^{'}}{p_{\mathrm{c}}^{'}} = \theta^{*}\frac{\mathrm{d}p_{\mathrm{y}}^{'}}{p_{\mathrm{y}}^{'}} \tag{18}$$

where, $p_{\mathrm{c}}^{'}$ is a hardening parameter and $p_{\mathrm{y}}^{'}$ is defined as (Roscoe and Burland 1968):

$$p_{\mathrm{y}}^{'} = p^{'} + \left(\frac{q}{M}\right)^{2}\frac{1}{p^{'}} \tag{19}$$

In the above, M is the slope of the critical state line in $p^{'}$-q space and $p^{'}$ and q are the effective mean stress and deviator stress, respectively.

The parameter θ^{*} is assumed to be (Ni et al., 2014):

$$\theta^{*} = \frac{1}{N\xi_1 + \xi_2} \tag{20}$$

where, ξ_1 and ξ_2 are experimental constants, and N is the number of cycles.

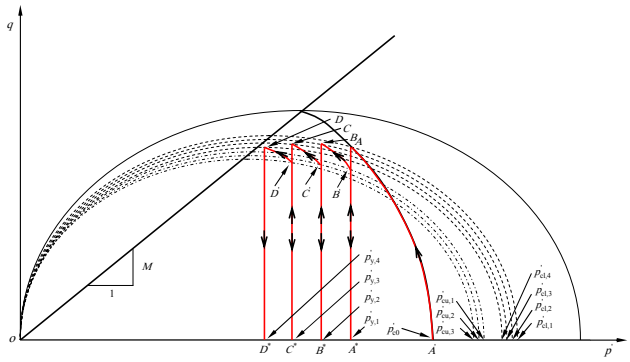

Figure 25. The stress path for cyclic loading (Ni et al. 2014, with permission from ASCE).

The stress path for normally and isotropically consolidated soils under cyclic loading is shown in Figure 25. When the stress path moves from point $A^{'}$ to point A during the first loading period, the soil behaves elastically. During the first unloading period, while the stress path travels from point A to A^{*}, the effective mean stress remains constant. The yield stress for the second cycle (i.e. yield stress after unloading) can be calculated through Eq. (18). During the first part of the second cycle, the stress path travels from point A^{*} to point $B^{'}$ and the soil behaves elastically. Subsequently, the stress path moves from point $B^{'}$ to B and the soil behaves plastically.

Undrained cyclic triaxial loading tests were conducted on reconstituted kaolinite specimens. The experimental results in terms of the axial strain and excess pore pressure are given in Figure 26. It can be observed that the excess pore pressure shows a sharp increase at the low cycle range and increases only modestly with a large number of cycles. The excess pore pressures reached a stable state for the specimens with Cyclic Stress Ratio (CSR) = 0.4 and 0.6, but for the specimen with CSR=0.8, a critical value of normalized excess pore pressure is reached after only a few cycles. It is also observed that failure cannot be assessed only on the basis of the normalized excess pore pressures. In fact, the failure of the two samples U_{03} and U_{12} is indicated by a sharp rise in axial strains at a critical

number of cycles. In contrast, for samples U_{01}, U_{02}, U_{10} and U_{11}, the final axial strains are still very small in the end.

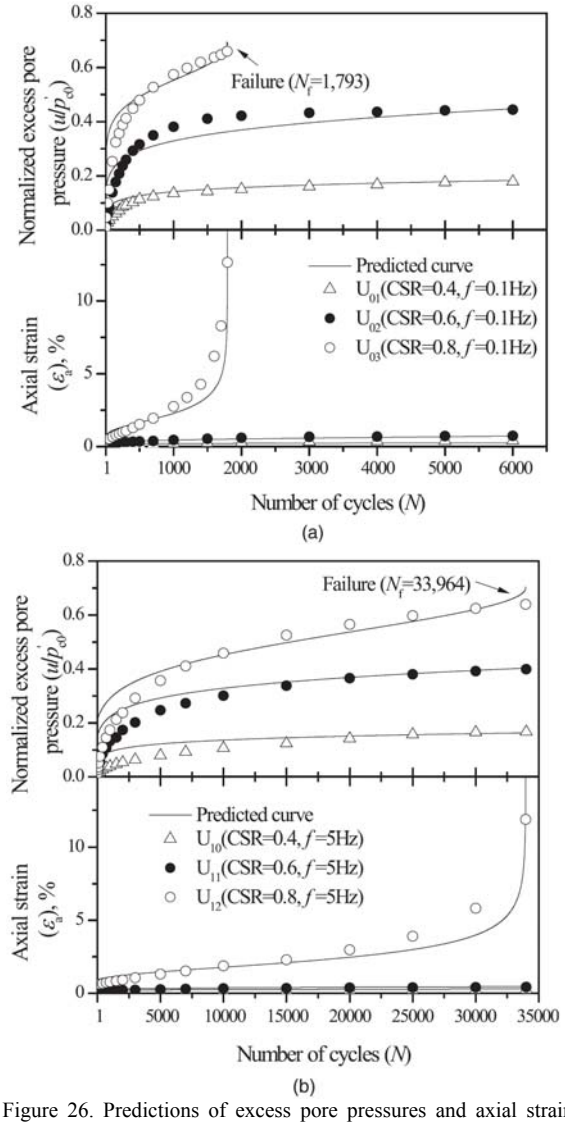

Figure 26. Predictions of excess pore pressures and axial strains: (a) f=0.1Hz, (b) f=5Hz (Ni et al. 2014, with permission from ASCE).

The simulation results are also plotted together with the experimental data in Figure 26. It can be observed that the model proposed accurately predicts the experimental behaviour both in terms of excess pore pressures and axial strains.

5. ANALYTICAL SOLUTION FOR RADIAL CONSOLIDATION WITH NATURAL (FIBRE) DRAIN BIODEGRADATION

Due to environmental concerns over the use of biodegradation resistant synthetic geomaterials and local availablility of materials, Natural PVD (NPVD) made from natural fibres such as jute and coir are increasingly being used, particulary in Asian countries. Since the first NPVD was introduced by (Lee et al. 1987), several investigations (Miura et al. 1995; Kim and Cho 2009; Saha et al. 2012) in the laboratory and field have identified that NPVDs have a potential to decay rapidly when exposed to harmful environments where particular bacteria (e.g., cellulose degrading bacteria) are available. Rapid degradation of natural fibres reduces the drainage characteristics of the drain hampering consolidation. Therefore, there is a critical need to evaluate the influence of drain biodegradation on soil consolidation.

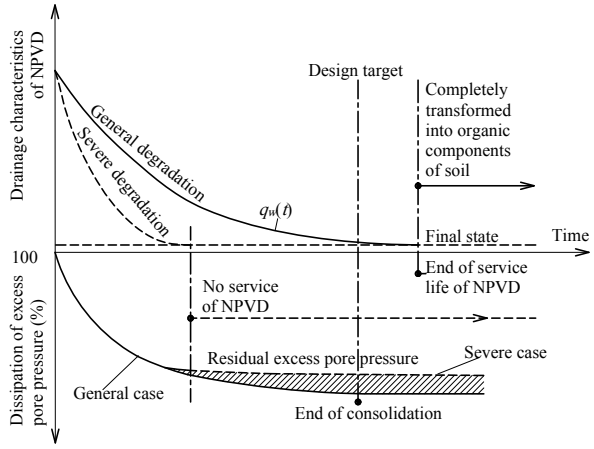

Figure 27 Degradation of drain discharge capacity with the corresponding consolidation of soil (Indraratna et al. 2016b, with permission from Elsevier).

Indraratna et al. 2016b present an analytical solution to equal strain radial consolidation where the discharge capacity of the drain reduces over time. The discharge capacity of drain begins to drop immediately reducing to a minimum level where natural fibres have completely transferred into organic components (Figure 27).

Radial consolidation with degrading discharge capacity can be described with the following governing equation:

$$u = \frac{\gamma_w}{2k_{h,a}} \frac{d_c^2}{4} \left(\mu_{n,s,a} + \mu_{q,a} \right) \frac{\partial \varepsilon}{\partial t} \tag{21}$$

In the above, $\mu_{n,s}$ is the parameter representing the geometric features of the drain while μ_q is a function of the drain discharge capacity $q_w(t)$ which is varying over time. The general solution of the ordinary differential equation Eq. (21) can be written as:

$$u(t) = u_o exp\left(-\int_0^t \frac{1}{f(t)} dt \right) \tag{22}$$

where the function $f(t)$ is given as follows:

$$f(t) = \chi \left(\mu_{n,s} + \frac{\lambda}{q_w(t)} \right) \tag{23}$$

where $\chi = (2\pi k_h l^2)/3$; $\lambda = d_e^2/(8c_h)$.

To illustrate how the solution can evaluate the influence of drain degradation on the consolidation of soil, an exponential degradation of discharge capacity is considered as follows:

$$q_w(t) = q_{wo} e^{-\omega t} \tag{24}$$

where ω is the decay coefficient representing the rate of the reduction in discharge capacity. The larger this coefficient, the faster the degradation of drain. Replacing Eq. (24) into Eq. (22) and then integrating yields:

$$\frac{u(t)}{u_o} = exp\left\{\frac{-8T_h}{\mu_{n,s}}\frac{1}{\chi\mu_{n,s}\omega}\left[\ln\left(\frac{\mu_{n,s}}{\mu_{qo}}+e^{\omega t}\right)-\ln\left(\frac{\mu_{n,s}}{\mu_{qo}}+1\right)\right]\right\} \quad (25)$$

The above is the exact solution to predict the radial consolidation of soil with respect to the exponential reduction in the drain discharge capacity. When ω approaches zero (no degradation), Eq. (25) reduces to the the conventional solution of Hansbo (1981) which considers q_w as constant over time.

Figure 28 shows how the proposed solution can capture the influence of biodegradation on the consolidation of soil. While excess pore pressure predicted by the conventional method can dissipate completely after nearly 500 days, for the degradable drain a residual excess pore presusre remains after the drain has completley degraded (e.g., 22% for ω = 0.02 day^{-1}). The retarded excess pore pressure dissipation only becomes apparent when q_w decreases to a certain level which is influenced by the consolidation coefficient c_h and the geometry of the unit cell (i.e., d_e and l). In this study, the value of drain discharge capacity where soil consolidation becomes retarded considerably is approximately 0.1 m^3/day.

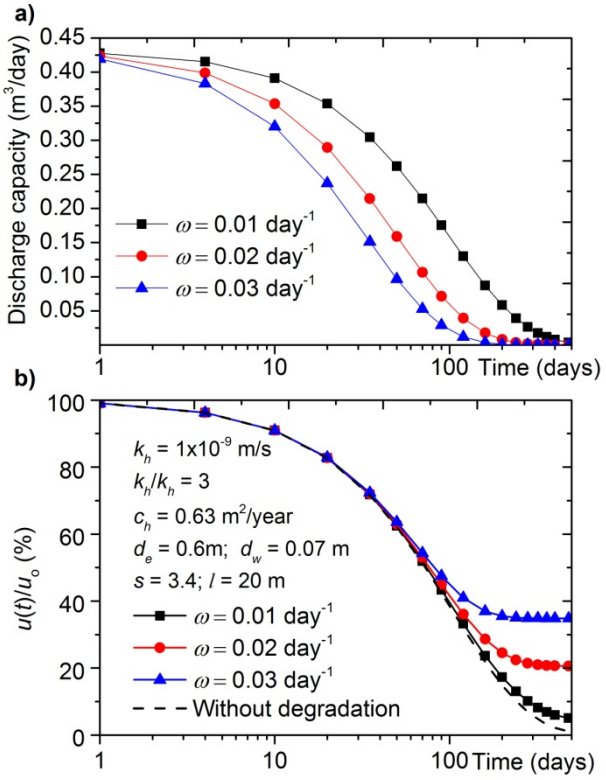

Figure 28. Influence of drain degradation on the consolidation of soil: a) Degradation with different decay rates; b) Corresponding dissipation of excess pore pressure (Indraratna et al. 2016b, with permission from Elsevier).

The proposed method is compared with previous studies, including (*i*) the laboratory work by Kim et al. (2011); and (*ii*) the analytical method by Deng et al. (2014). A degradation curve with ω = 0.259 day^{-1} is obtained from the experimental result made by Kim et al. (2011). Figure 29 shows a good agreement between the analytical and experimental methods. The consolidation curves predicted by the current method and one proposed by Deng et al. (2014) are almost identical. There is only a subtle difference between them because Deng et al. (2014) solves the governing equation by an approximate approach while an exact solution is applied in this study. Furthermore, Deng et al. (2014) only consider the exponential degradation of drain permeability whereas the current study introduces a general form of drain discharge capacity and incorporates it into the governing equation for excess pore pressure dissipation, resulting in a more flexible approach which can accommodate various reduction forms of drain discharge capacity.

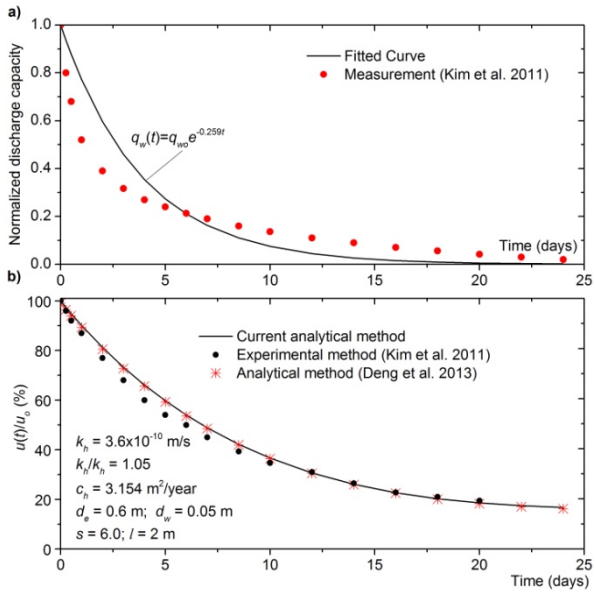

Figure 29. Comparison of the proposed method with previous studies (Indraratna et al. 2016b, with permission from Elsevier) .

6. NUMERICAL ANALYSIS –PLANE STRAIN CONVERSION

The majority of models in Sections 2, 3, and 5 above consider an idealized single drain in an axi-symmetric soil cylinder subject to vertical loads. The most common technique to study full embankment behaviour is the finite element method. For multi-drain simulation, plane strain finite element analysis can be readily adapted to most field situations (Hird et al. 1995, Indraratna and Redana 2000; Indraratna et al. 2005a). Nevertheless, realistic field predictions require that the axi-symmetric properties be converted to an *equivalent* 2D plane strain condition, especially the permeability coefficients and drain geometry. Plane strain analysis can also accommodate vacuum preloading in conjunction with vertical drains (e.g. Gabr and Szabo 1997). Indraratna et al. (2005b) proposed an equivalent plane strain approach to simulate vacuum pressure for a vertical drain system with modification to the original theory introduced by Indraratna and Redana (1997), as shown in Figure 30.

Equivalent plane strain conditions can be fulfilled in three ways:

(1) Geometric approach where the PVD spacing varies, but the soil permeability remains constant;

(2) Permeability approach where the equivalent permeability coefficient is determined while the drain spacing remains unchanged;

(3) Combined permeability and geometric approach where plane strain permeability is calculated based on a convenient space between the drains.

Indraratna et al. (2005b) proposed an average degree of consolidation for plane strain by assuming that the plane strain cell (width of 2*B*), the half width of the drain b_w and the half width of the smear zone b_s may be kept the same as their axi-symmetric radii r_w and r_s, respectively. This implies that b_w=r_w

and b_s=r_s (Figure 30). To excess pore pressure can be determined from:

$$\frac{\bar{u}}{\bar{u}_0} = \left(1 + \frac{p_{0p}}{\bar{u}_o}\frac{(1+k_1)}{2}\right)\exp\left(-\frac{8T_{hp}}{\mu_p}\right) - \frac{p_{0p}}{\bar{u}_0}\frac{(1+k_1)}{2} \quad (26a)$$

and

$$\mu_p = \left[\alpha + (\beta)\frac{k_{hp}}{k'_{hp}}\right] \quad (26b)$$

where $\bar{u}_0$ = the initial excess pore pressure, $\bar{u}$ = the pore pressure at time t (average values) and T_{hp} = the time factor in plane strain, and k_{hp} and k'_{hp} are the equivalent undisturbed horizontal and corresponding smear zone permeability, respectively. The geometric parameters α and β are given by:

$$\alpha = \frac{2}{3} - \frac{2b_s}{B}\left(1 - \frac{b_s}{B} + \frac{b_s^2}{3B^2}\right) \quad (27a)$$

$$\beta = \frac{1}{B^2}(b_s - b_w)^2 + \frac{b_s}{3B^3}\left(3b_w^2 - b_s^2\right) \quad (27b)$$

At a given level of effective stress, and at each time step, the average degree of consolidation for the axisymmetric ($\bar{U}_p$) and equivalent plane strain ($\bar{U}_{p,pl}$) conditions are made equal.

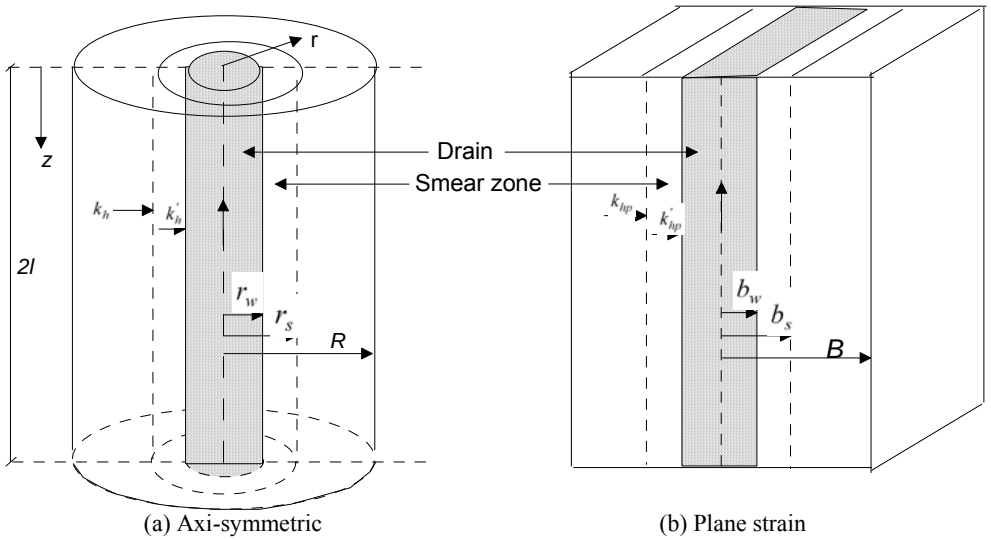

(a) Axi-symmetric (b) Plane strain

Figure 30. Conversion of an axisymmetric unit cell into plane strain condition (Indraratna et al. 2005b, with permission from ASCE).

By making the magnitudes of R and B the same, Indraratna et al. (2005a) presented a relationship between k_{hp} and k'_{hp}. The smear effect can be captured by the ratio between the smear zone permeability and the undisturbed permeability, hence:

$$\frac{k'_{hp}}{k_{hp}} = \frac{\beta}{\frac{k_{hp}}{k_h}\left[\ln\left(\frac{n}{s}\right) + \left(\frac{k_h}{k'_h}\right)\ln(s) - 0.75\right] - \alpha} \quad (28)$$

Ignoring the effects of smear and well resistance in the above expression would lead to the simplified solution proposed earlier by Hird et al. (1992):

$$\frac{k_{hp}}{k_h} = \frac{0.67}{[\ln(n) - 0.75]} \quad (29)$$

Indraratna et al. (2005b) compared two different distributions of vacuum along a single drain for the equivalent plane strain (2D) and axisymmetric conditions (3D). Varying the vacuum pressure in PVDs installed in soft clay would be more realistic for long drains, but a constant vacuum with depth is justified for relatively short drains.

7 CASE HISTORIES

Compendiums edited by Indraratna and Chu (2005e) and Indraratna et al. (2015c) describe many successful ground improvement projects. This section looks at two PVD-vacuum case histories from Australia and one from China which have been modelled using techniques described above.

7.1 *Ballina Bypass*

The Pacific Highway on Australia's East coast linking Sydney and Brisbane bypasses the town of Ballina. This bypass route has to cross a floodplain consisting of highly compressible and saturated marine clays up to 40 m thick. At one bridge abutment combined vacuum and surcharge preloading with PVDs was selected to shorten the consolidation time and stabilise the deeper clay layers. To investigate the effectiveness of this approach, a trial embankment was built north of Ballina, where 34 mm diameter circular PVD at 1.0m spacing were installed in a square pattern. The vacuum system consisted of PVDs with an air and water tight membrane, horizontal transmission pipes, and a heavy duty vacuum pump. Transmission pipes were laid horizontally beneath the membrane to provide uniform distribution of suction through the drainage blanket. The boundaries of the membrane were embedded in a peripheral trench filled with soil-bentonite to ensure air tightness. Figure 31 presents the instrument locations, including surface settlement plates, inclinometers and piezometers. The piezometers were placed 1m, 4.5m, and 8m below the ground

level, and eight inclinometers were installed at the edges of the embankment. The embankment area was then divided into Section A (no vacuum pressure), and Section B that was subjected to vacuum pressure and surcharge fill. As the layers of soft clay ranged 7m to 25 m thick (Table 2), the embankment varied from 4.3m to 9.0m high, to limit the post-construction settlement. A vacuum pressure of 70 kPa was applied at the drain interface and removed after 400 days. The geotechnical parameters of the three subsoil layers obtained from standard odometer tests are given in Table 3.

The soil profile with its relevant properties is shown in Figure 32. A soft silty layer of clay approximately 10m thick was underlain by a moderately stiff and silty layer of clay located 10-30m deep, which was in turn underlain by firm clay. The groundwater was almost at the ground surface. The water content of the soft and medium silty clay varied from 80 to 120%, which was generally at or exceeded the liquid limit, ensuring that the soils were fully saturated. The field vane shear tests indicated that the shear strength was from 5-40 kPa. The compression index ($C_c/(1+e_0)$) determined by standard oedometer testing was between 0.30-0.50.

Settlement and associated pore pressure recorded by the settlement plates and piezometers are shown in Figure 33, along with the embankment construction schedule. The actual suction varied from -70 kPa to -80 kPa, and no air leaks were encountered. Suction was measured by miniature piezometers embedded inside the drains.

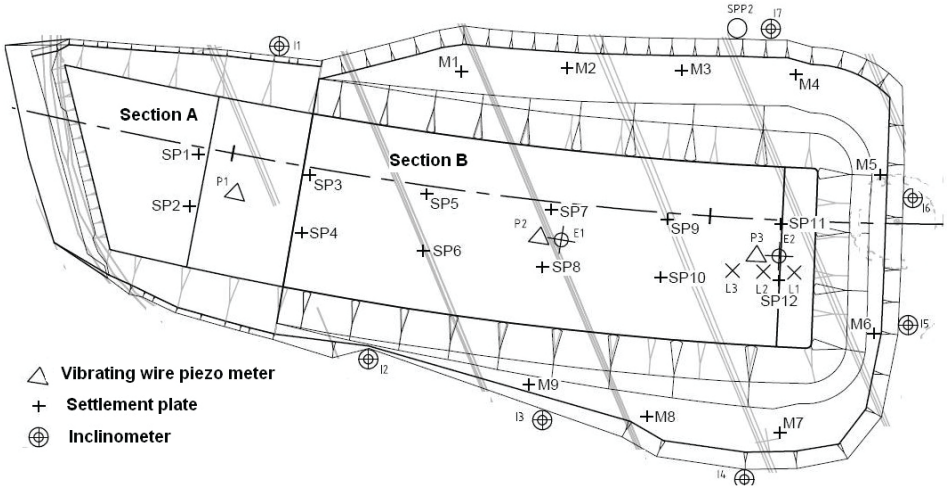

Figure 31. Instrumentation layout for the test embankments at Ballina Bypass (Indraratna et al. 2012, with permission from ICE).

Table 2: Bottom level of soft clay layer at each settlement plate (Indraratna et al. 2012, with permission from ICE).

Settlement plate	SP1, SP2	SP3,SP4	SP5,SP6	SP7, SP8	SP9, SP10	SP11, SP12
Bottom level of soft clay layer (m-RL)	2.7-6.7	6.7-9.7	9.7-11.7	11.7-14.7	14.7-17.7	20.7-24.7

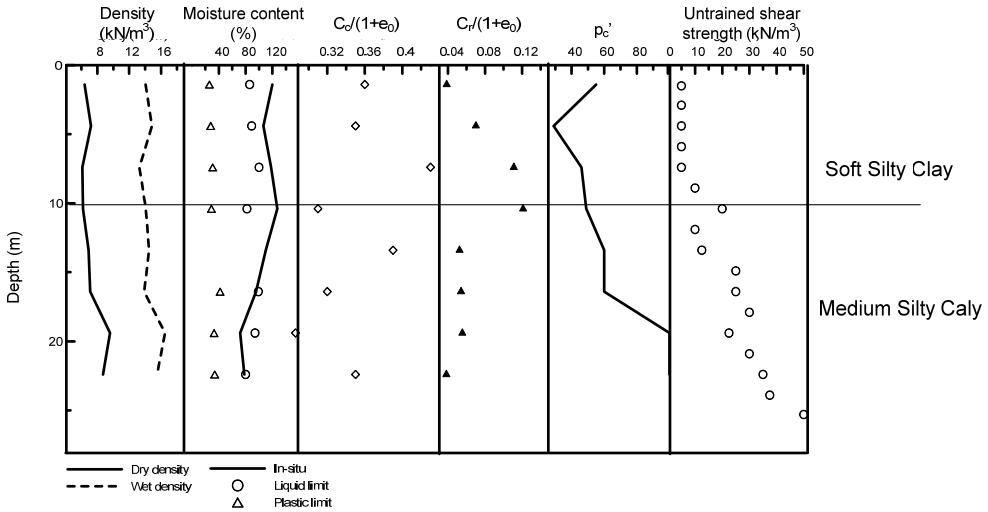

Figure 32. General soil profile and properties at Ballina Bypass (Indraratna et al. 2012, with permission from ICE).

Table 3: Soil parameters at SP12 (Indraratna et al. 2012, with permission from ICE).

Depth (m)	Soil Type	λ	κ	γ (kN/m^3)	e_0	$k_{h,ax}$ (10^{-10} m/s)	OCR
0.0-0.5	Clayey silt	0.57	0.06	14.5	2.9	10	2
0.5-15.0	Silty Clay	0.57	0.06	14.5	2.9	10	1.7
15.0-24.0	Stiffer Silty Clay	0.48	0.048	15.0	2.6	3.3	1.1

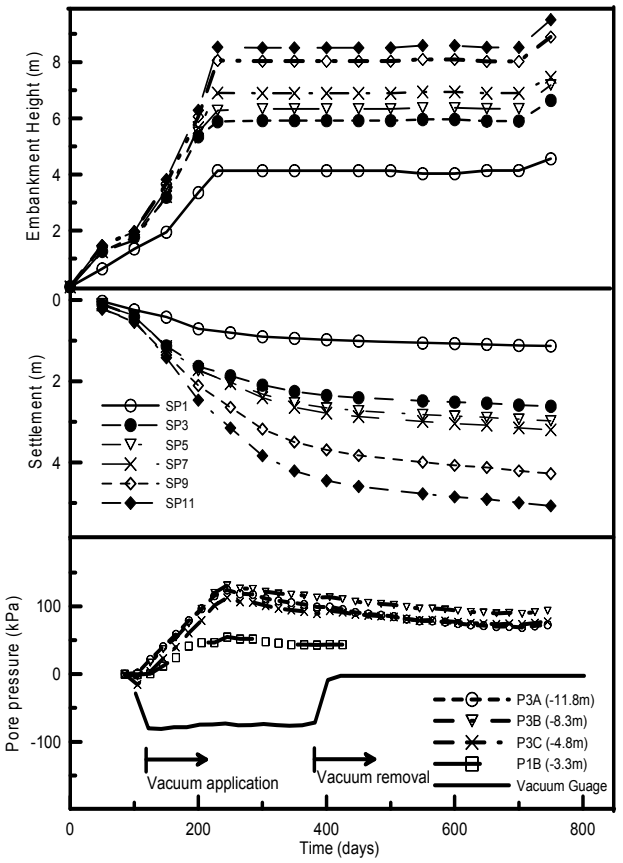

Figure 33. Embankment stage construction with associated settlements and excess pore pressures (Indraratna et al. 2012, with permission from ICE).

Lateral displacement at the tow of the embankment needed to be examined carefully, particularly in the vacuum area where the surcharge loading was raised faster than that at the non-vacuum area. The soil properties and lateral displacement plots before and after vacuum are shown in Figure 34. Inclinometer I1 was installed in the no-vacuum area, whereas inclinometers I2-I7 were located at the edge of the vacuum area. Here the lateral displacement subjected to vacuum was smaller even though the embankments were higher. In Figure 34b the plot of lateral displacement normalised to embankment height shows that the vacuum pressure undoubtedly has reduced lateral displacement.

2D and 3D single drain analyses were used to compute the settlement at location SP-12. Typical 2D finite element mesh is shown in Figure 35a. The construction history and measured settlement at the settlement plate SP-12 are shown in Figure 40b & c. Here the clay was assumed to be 24m thick, based on CPT data. The analytical pattern was similar to Indraratna et al. (2005a). The predictions from 2D and 3D analyses agreed with the measured data, where the rate of settlement increased significantly after a vacuum was applied (Figure 35c).

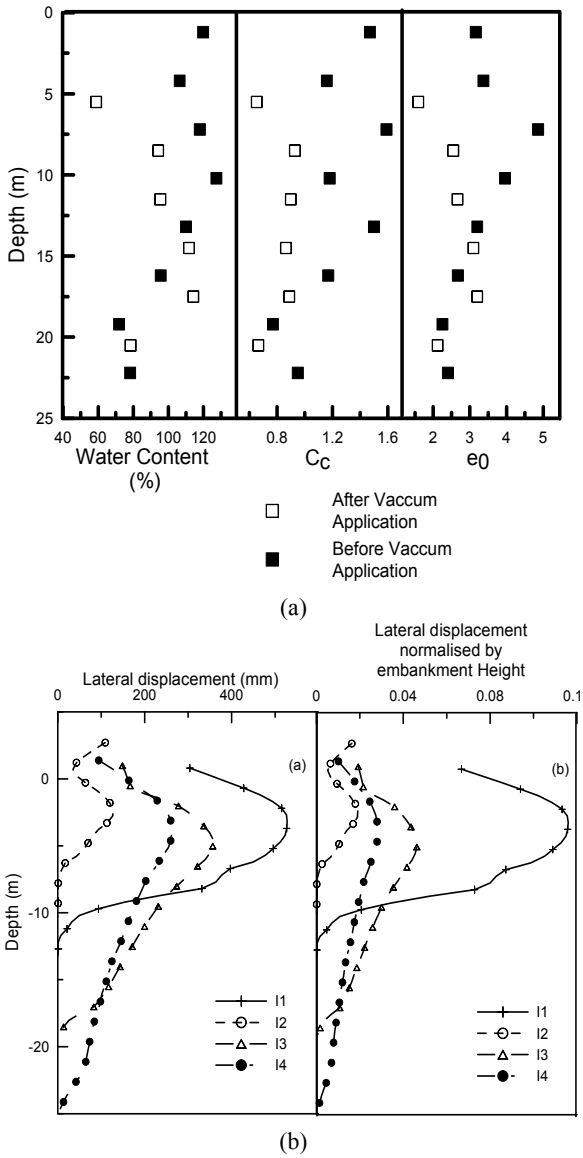

Figure 34. (a) Soil properties before and after vacuum application; and (b) Measured lateral displacement and lateral displacement normalised with embankment height (Indraratna et al. 2012, with permission from ICE).

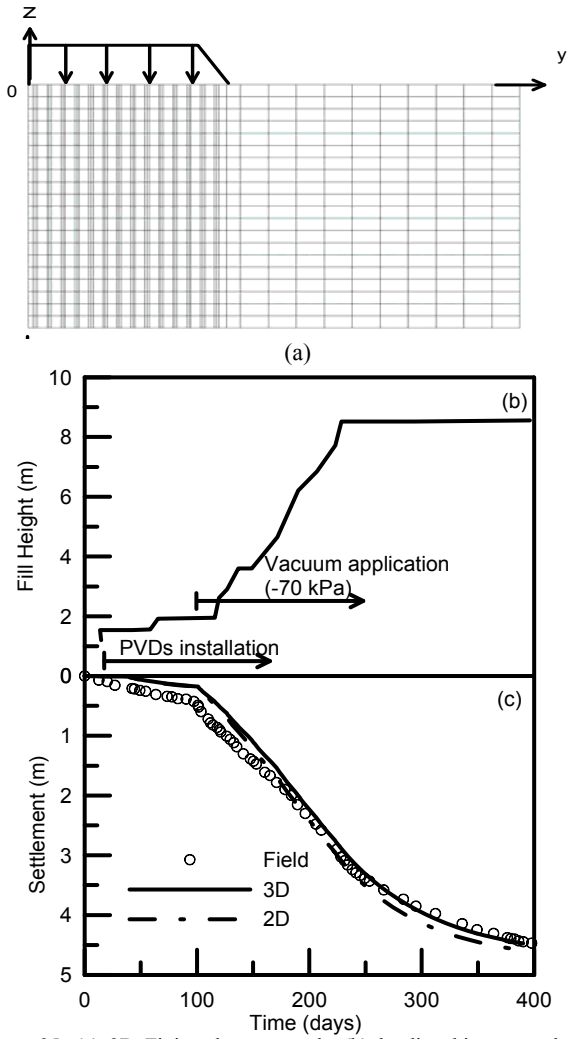

Figure 35. (a) 2D Finite element mesh; (b) loading history; and (c) consolidation settlements for settlement plate SP-12 (Indraratna et al. 2012, with permission from ICE).

7.2 *Port of Brisbane*

The Port of Brisbane is located at the mouth of the Brisbane River at Fisherman Islands, Queensland Australia. An expansion of the Port includes a 235ha area to be progressively reclaimed and developed over the next 20 years using dredged materials from the Brisbane River and Moreton Bay shipping channels. The site contains compressible clays over 30 m thick. At least 7 m of dredged mud capped with 2 m of sand was used to reclaim the sub-tidal area. With surcharge alone, the complete consolidation of the soft deep clay deposits may take in excess of 50 years, with associated settlements 2.5-4 m likely. To reduce the consolidation period, the method of PVD and surcharge or PVD combined with vacuum pressure (at sites where stability is of a concern) was chosen to be trialled (Indraratna et al., 2011). Three contractors trialed prefabricated drains and surcharge using respective membrane and membraneless vacuum systems. Figure 36 shows the final layout of the typical trial area with the design specifications for each area. The relevant soil properties are given in Table 1.

To compare two locations with a different loading history, the lateral displacement normalised by the applied effective stress at two inclinometer positions (MS24 and MS34) are plotted in Figure 37. It is clear that the lateral displacements are largest in the upper Holocene shallow clay depths and are insignificant at shallow depths, say below 10m. From this limited inclinometer data, the membrane-less BeauDrain system (MS34) had controlled the lateral displacement more effectively than the surcharge only section (MS24). Settlement and excess pore water pressure predictions and field data for a typical settlement plate (TSP3) are shown in Figure 38. The predicted settlement curve agrees with the field data. The excess pore water pressures were more difficult to predict than settlement, but they did indicate a slower rate of dissipation in the Holocene clays in every section monitored, in spite of the PVDs. From the perspective of stability, the incremental rate of change of the lateral displacement/settlement ratio (μ) with time can be plotted as shown in Figure 39. This rate of change of μ can be determined for relatively small time increments where a small and decreasing gradient can be considered to be stable with respect to lateral movement, while a continuously increasing gradient of μ reflects potential lateral instability. In Figure 39, the gradient in the non-vacuum area VC3 increased initially, which could be attributed to the final surcharge loading placed quickly, while the clay was still at early stages of consolidation. However, as the PVDs become fully active and settlement increased at a healthy rate, the gradient of μ decreased, as expected. In general, Figure 39 illustrates that the vacuum pressure provides a relatively unchanging gradient of μ with time.

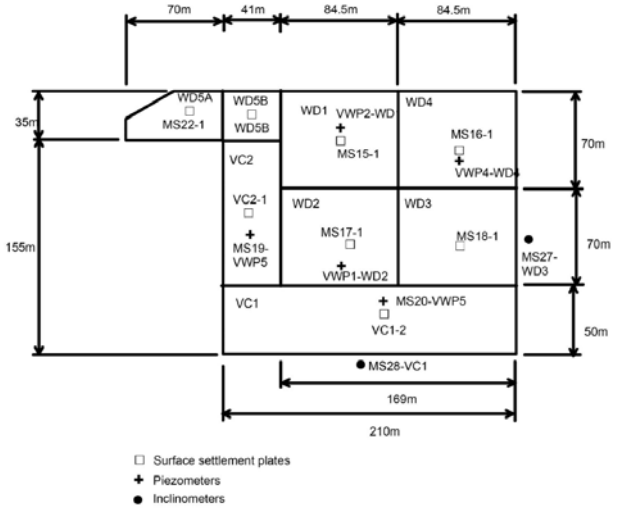

Figure 36. S3A Trial Area – Layout and detail design specifications (Indraratna et al., 2011, with permission from ASCE).

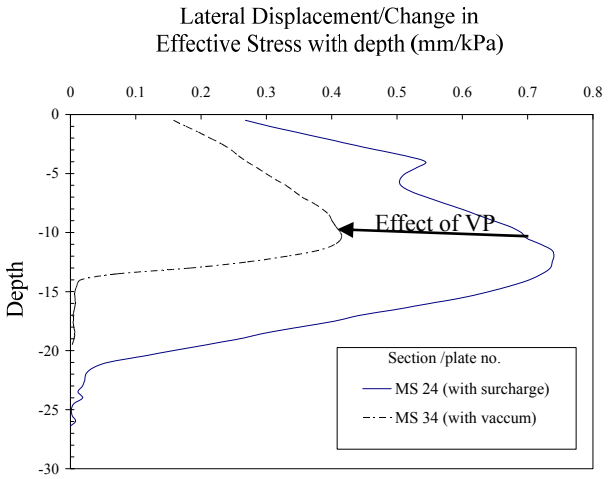

Figure 37. Comparison of lateral displacements in vacuum and non-vacuum areas (Indraratna, 2010, with permission from AGS).

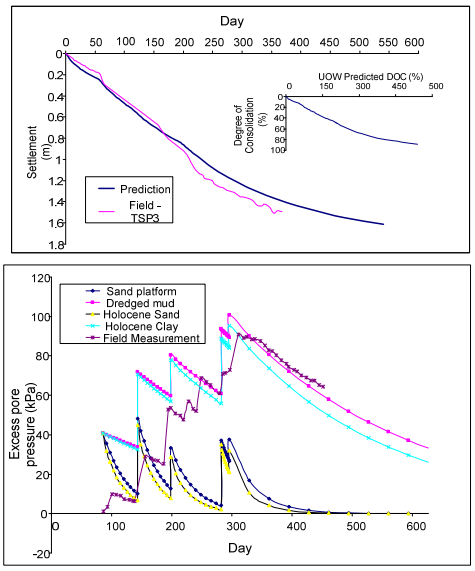

Figure 38. (a) Settlement; and (b) excess pore water pressure predictions and field data for a typical settlement plate location. (Indraratna, 2010, with permission from AGS).

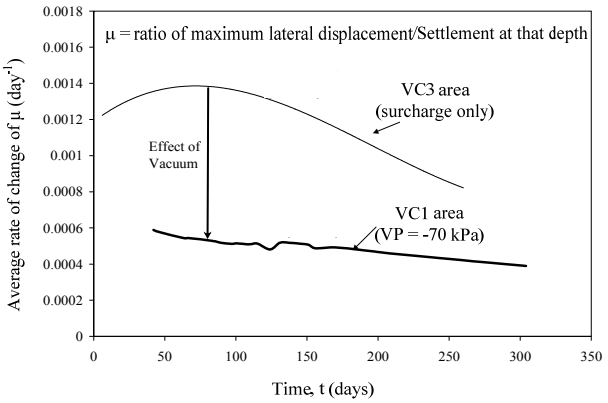

Figure 39. Rate of change of lateral displacement/settlement ratio with time (Indraratna, 2010, with permission from AGS).

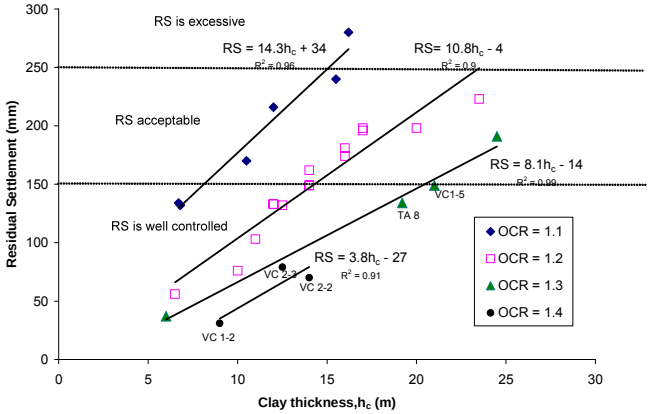

Figure 40. Effect of OCR and clay thickness on residual settlement. (Indraratna, 2010, with permission from AGS).

Figure 40 provides approximately linear relationships between the long term residual settlement (RS) and the clay thickness of clay for an initial over-consolidation ratio (OCR) from 1.1 to 1.4, and for a degree of consolidation (DOC) that exceeding 80%. The reduced settlement (RS) was determined based on the theory of secondary consolidation employing the secondary compression index C_α (Table 1). More details on the computation of RS are given by Mesri and Castro (1987), Bjerrum (1967) and Yin and Clark (1994). As expected, when the OCR increases, the RS decreases substantially. In general, as the thickness of Holocene clay increased, the RS also increased. The corresponding regression lines and best–fit equations are also shown in Figure 40. In particular, the vacuum consolidation locations (VC1-2, VC2-2 and VC2-3) show a considerably reduced RS at an OCR approaching 1.4, which is well below the permissible limit of 250mm. At an OCR of approximately 1.3, the residual settlement associated with membraneless consolidation (TA8) and membrane type (VC1-5) were also small.

Table 1. Typical Soil Properties (Indraratna, 2010, with permission from AGS).

Soil layer	Soil type	γ_t (kN/m^3)	$C_c/(1+e_0)$	c_v(m^2/yr)	c_h(m^2/yr)	k_h/k_s	$s=d_s/d_w$	$C_\alpha/(1+e_0)$
1	Dredged Mud	14	0.3	1	1	1	1	0.005
2	Upper Holocene Sand	19	0.01	5	5	1	1	0.001
3	Upper Holocene Clay	16	0.18	1	2	2	3	0.008
4	Lower Holocene Clay	16	0.235	0.8	1.9	2	3	0.0076

7.3 *Tianjin Port*

Tianjin port is approximately 100km from Beijing, China. The top 15m of soil at this site was soft to very soft and needed to be improved using a preloading surcharge of more than 140kPa (Rujikiatkamjorn et al. 2008). To avoid any stability problems (high lateral yield) associated with a high surcharge embankment, a fill height corresponding to 50 kPa plus a vacuum pressure of 80 kPa were applied on top of the 20 m thick soft soil layer in conjunction with PVDs installed at 1.2 m spacing in a square pattern. The conversion method proposed by Indraratna et al (2005b) was used for the 2D plane strain FEM analysis (

Figure 41), and the finite element program (ABAQUS) was used to simulate the 3D multi-drain analysis (Figure 42), employing the Biot coupled consolidation theory.

In terms of settlement, excess pore pressure, and lateral displacement, the numerical results from the equivalent 2D and true 3D analyses were quite similar (Figure 43 andFigure 44). This proves that, the equivalent plane strain (i.e. 2D) analysis is usually sufficient from a computational point of view,

especially for multi-drain analysis of large projects where a 3D model would be more time consuming. From a practical point of view, the height of surcharge fill can be reduced by applying vacuum preloading to achieve the same rate and degree of consolidation. Applying a surcharge pressure after the initial vacuum preloading could also reduce excessive inward lateral movement near the toe of the embankment (Rujikiatkamjorn et al. 2008; Rujikiatkamjorn et al. 2007).

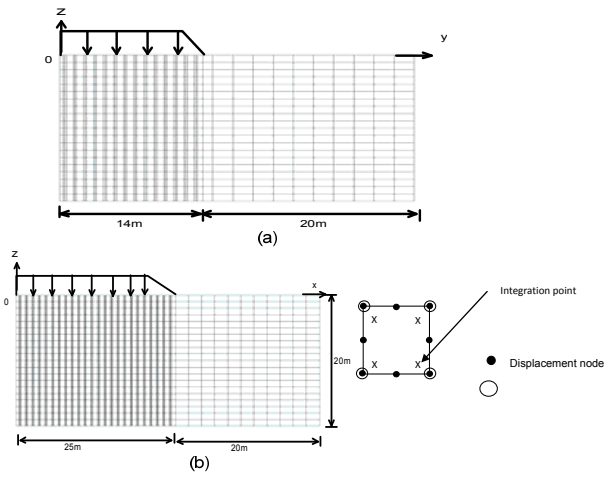

Figure 41. 2D finite-element mesh: (a) x=0 plane; (b) y=0 plane (Rujikiatkamjorn et al. 2008, with permission from ASCE).

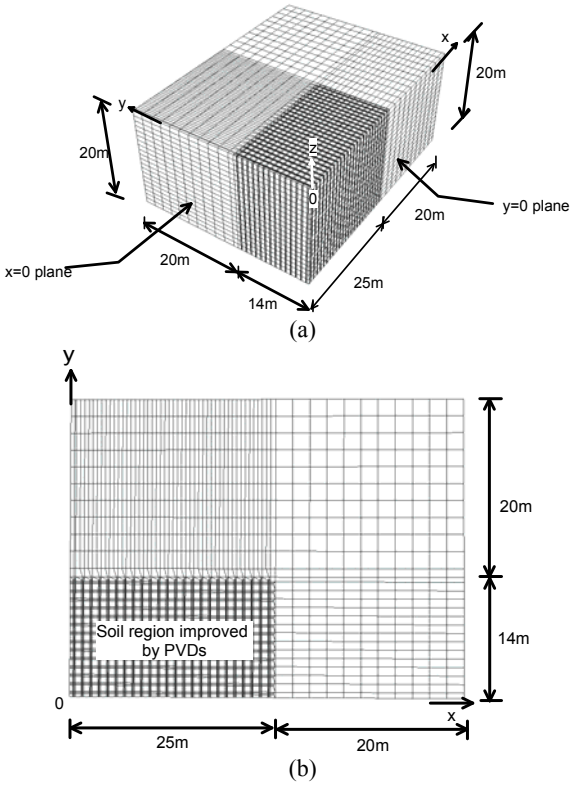

Figure 42. 3D finite-element mesh: (a) Isometric view; (b) top view (Rujikiatkamjorn et al. 2008, with permission from ASCE).

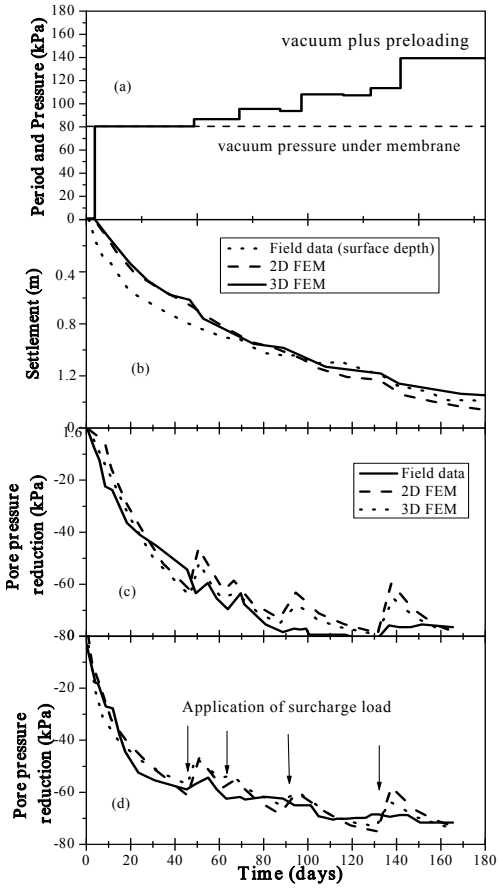

Figure 43. Measurements of Tianjin Port: (a) Loading history; (b) consolidation settlement; (c) pore pressure variation at 0.25m away from embankment centreline (Section II): 5.5m depth; (d) pore pressure variation at 0.25m away from embankment centreline (Section II): 11.0m depth (arrows indicate items when surcharge loads were applied) (Rujikiatkamjorn et al. 2008, with permission from ASCE).

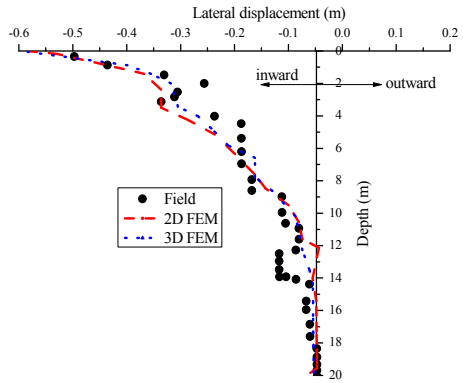

Figure 44. Lateral displacement at embankment toe (Section II at 180th day) (Rujikiatkamjorn et al. 2008, with permission from ASCE).

8. FIELD OBSERVATION OF RETARDED PORE PRESSURE DISSIPATION

It has been observed in various case studies that in spite of PVDs, excess pore water pressures do not always dissipate as fast as one expects, even when the load remains constant or removed. In visco-plastic soils, the high lateral yield causing stress redistribution can increase the total stress hence the pore water pressure in some regions of the clay foundation. Mandel-Cryer effect has been cited by some to explain this phenomenon, where coupling effects in interconnected fluid-saturated pores suggest that when a porous material is under

stress, the corresponding non-uniform stress redistribution and associated changes in pore fluid pressure cause soil deformation. The time-dependent fluid flow will also generate a non-uniform pore pressure distribution that effect corresponding stresses and strains while giving rise to increased pore water pressure in some soil regimes that can be captured by strategic locations of piezometers. Numerical analyses conducted on highly viscous soils can provide evidence that retardation of pore water pressure dissipation is partially attributed to the pore pressures created by non-uniform stress re-distributions and resulting anisotropic yielding especially beneath soft clay embankments. Moreover, in certain find grained soils the clogging of piezometers filters, extreme reduction of the lateral soil permeability, and damage to or corrosion of piezometer tips over time can affect piezometer readings. A typical example is shown in Fig. 45 where the anticipated perfect drainage behaviour will not be achieved irrespective of the drain spacing.

Moreover, in highly organic or pyritic (acid sulphate) soil floodplains prevalent in coastal Australia, partial clogging of piezometers with time caused by chemical precipitation (e.g. iron oxides), acidophilic anaerobic bacteria-induced gas bubbles (cavitation), corrosion of measuring tips and growth of bio-slimes may also inhibit pore pressure dissipation (Indraratna et al., 2010, www.corrosionpedia.com/definition/1339/bacterial-anaerobic-corrosion).

The routine tidal effects and flash flooding in low-lying coastal floodplains also influence the field pore water pressures, unless proper calibration can be conducted based on local geo-hydraulic and meteorological records. In past years, malfunctioning piezometers examined after about 1.5-2 years from the Shoalhaven pyritic floodplain, NSW (south of Sydney) have indicated fines accumulation (partial clogging) and deterioration of filter tips, with evidence of medium-high levels of anaerobic bacteria (thiobacillus ferrooxidans) that even under water can catalyse chemical precipitation and biological growth under low pH (<6) conditions. Precipitation of iron oxide may occur within the granular drainage medium surrounding the piezometer tips leaving reddish-brown rust deposits armouring the particles and partially filling the pores (see Fig. 46). This implies that for long-term monitoring, standpipe piezometers that can be maintained by backwashing may be beneficial to be used in tandem with vibrating wire piezometers (VWP), albeit the expected higher time-lag of the former. The main disadvantage of the VWPs in such soils is that they cannot be maintained (flushed) once installed. The excess pore water pressure dissipation for selected case histories (a) Port of Brisbane (POB), Queensland (b) Muar clay, Malaysia, (c) Pacific Highway, Ballina Bypass and, (d) Suwarnabhumi International Airport (SBIA), Thailand, have been plotted in Figure 47(a). There is an acceptable steady rate of pore pressure dissipation for two cases (for e.g. POB and SBIA) but a sudden total retardation of pore pressure dissipation is observed for the site selected from Pacific Highway (Ballina Bypass). Compared to the Port of Brisbane site, the Ballina bypass site is located in an acid sulphate floodplain area with a relatively high organic content (4-6%) and low groundwater pH (< 5.5). This implies that in the longer term, subsurface drainage media and piezometer surrounds can experience some degree of clogging when installed in acid sulphate (pyritic) soils. Such apparent clogging (retarded pore pressure dissipation) in certain soil conditions may be described by a three-zone trend as shown in Fig. 47(b). At the initial stage of soil consolidation where accurate measurements are critical up to a peak, the piezometers may function reliably. In the second intermediate stage, the filters may become partially clogged and a significantly increased time-lag may be required to establish the equilibrium at the soil-filter interface. In the third stage, filter clogging may become more substantial to the extent that excess pore water pressure readings may remain almost constant, as the 'hydraulic connection' to the measuring tip is obstructed. It seems that this type of pore pressure trends have been observed from time to time along the Australian northern and eastern coastal areas that are affected by acid sulphate soil conditions within relatively shallow depths of the upper Holocene clay.

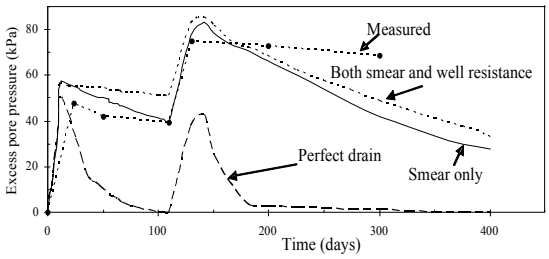

Figure 45 Excess pore water pressure variation at piezometer location, P6 (after Indraratna & Redana, 2000; Indraratna & Chu, 2005)

Figure 46 Precipitation of iron oxide in granular medium

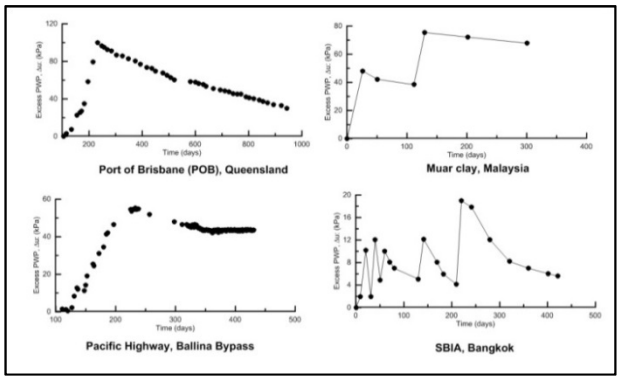

(a)

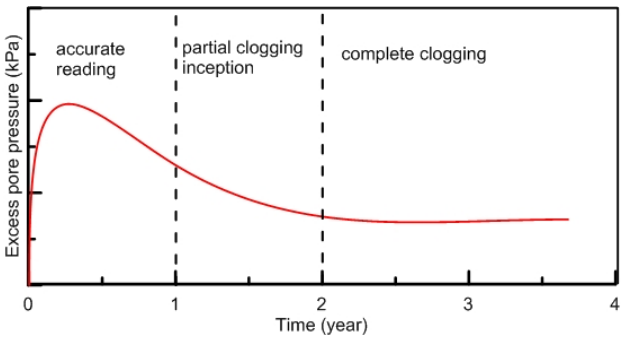

(b)

Figure 47 (a) Selected cases of excess pore pressure dissipation trends (b) A hypothetical model for potential long-term clogging of piezometers and subsurface drainage media in the absence of flushing.

9. CONCLUSION

The application of PVDs combined with vacuum and surcharge preloading has become common practice, and is now considered to be one of the most effective ground improvement techniques for soft clays worldwide. Analytical and numerical modelling of vacuum preloading is still a developing research area, especially considering the complexities at the soil-drain interface, biodegradation of natural fibre drains and the effects of PVD bending with settlement in shallow depths. There has always been a discrepancy between the predictions and observed performance of embankments stabilised with vertical drains and vacuum pressure. This discrepancy can be attributed to numerous factors such as the uncertainty of soil properties, the effect of smear and soil destructuration, inaccurate assumptions of soil behaviour and vacuum pressure distribution, effects of large strains and the improper conversion of axisymmetric condition to plane strain (2D) analysis of multiple drains.

Vacuum assisted consolidation has successfully been used for large scale projects on very soft soils in reclamation areas. The extent of surcharge fill can be decreased to achieve the same amount of settlement and the lateral yield of the soft soil can be controlled by PVDs used in conjunction with vacuum pressure. The effectiveness of this system depends on (a) the air tightness of the membrane, (b) the seal between the edges of the membrane and the ground surface, and (c) the soil conditions and location of the ground water level. The exact role of membrane type and membraneless systems for vacuum preloading requires detailed evaluation. In the absence of a comprehensive and quantitative analysis, the study of suitable methods to apply vacuum preloading becomes imperative, experimentally, numerically and more significantly in the field.

Performance of vacuum assisted consolidation has been studied using large-scale consolidometers to obtain more realistic parameters, including the correct smear zone characteristics, the distribution of vacuum along the length of the drain, as well as soil and drain properties. Conventional small-scale equipment (e.g. Rowe cell) cannot capture these parameters. The equivalent radius of the smear zone can generally be taken as 2-3 times larger than the equivalent radius of the mandrel and the soil permeability in the smear zone is usually smaller than the undisturbed zone by a factor of 1.5-2. In the field where there are no boundary effects such as in laboratory equipment, the actual smear zone can be larger. In order to predict the correct field behaviour, the smear zone effects and the soil disturbance need to be evaluated in the field using soil sampling and field piezometer data, while recognizing the limitations of the laboratory equipment where the depth and width are often inadequate to eliminate adverse boundary and scale effects. A suitable drain spacing pattern in the field should be determined to avoid the detrimental effects of overlapping smear zones when drains are spaced too closely.

Analytical modelling of vertical drains that include vacuum preloading under axisymmetric and plane strain conditions that simulate the consolidation of a unit cell surrounding a single vertical drain has been developed. The effects of vacuum propagation along the length of a drain, the nonlinear soil properties and the occurrence of non-Darcian flow conditions have been incorporated in the proposed solutions to obtain a more realistic prediction. Large strain analysis based on a convective coordinate system showed that that the large strain effects would make a notable difference in predicting the settlement induced by very large preloading (greater than 120 kPa), while for most traditional road embankments the conventional small strain solution is acceptable.

In large construction sites where many PVDs are installed, a 2D plane strain analysis is usually sufficient to model embankment behaviour. The proposed conversion from axi-symmetric to a plane strain condition agreed with the data available from case histories, including Port of Brisbane in Australia. These simplified plane strain methods can be readily incorporated in numerical (FEM) analysis. The conversion procedure from 3D to 2D based on the correct transformation of permeability and vacuum pressure, ensure that the time-settlement curves are the same as the true 3D analysis. However, at specific boundaries and corners where sudden change in properties and terrain characteristics occur, and also at curved sections (e.g. road and rail embankments), the 3D analysis remains as the only choice where plane strain conditions cannot be assumed. Field behaviour and model predictions indicate that the efficiency of vertical drains depends on the magnitude and distribution of vacuum pressure, the extent of smear caused by the vertically penetrating mandrel, and drain discharge capacity. Drain discharge capacity is particularly relevant for natural fibre drains which may decay over time. Provided that consolidation can occur prior to significant decay, these natural fibre-based PVD may be a more environmentally friendly than conventional, non-decaying synthetic drains.

From a practical point of view, vacuum preloading can reduce surcharge fill heights while achieving similar, if not faster, consolidation times compared to fill-only surcharge embankments. Vacuum systems eliminate the need for a high embankment surcharge load, but air leaks must be prevented as much as possible. Vacuum consolidation is ideal where lateral displacements must be strictly controlled such as at marine boundaries (e.g. Port of Brisbane) where environmental and aquatic regulations are stringent to prevent turbidity of water. Apart from road embankments, PVDs will also help stabilise rail tracks in coastal areas containing a high percentage of clayey subgrades. It has been shown that short PVDs can be used under rail tracks to improve stability by dissipating excess cyclic pore pressure and curtailing lateral displacement.

Dynamic triaxial testing with cyclic stress ratios and frequencies representing fast heavy haul trains is imperative to study the phenomenon of subgrade slurry (mud pumping) and undrained instability in low-lying estuarine soils. The testing conducted at the University of Wollongong over the past decade indicates that rapid dissipation of dynamic pore water pressures is vital for ensuring the stability of saturated subgrade. In this regard, the study of PVD under cyclic loading is considered vital and the manufacturing of custom-made geosynthetic drains for cycling loading conditions representing fast moving freight trains, will need to be evaluated and established.

Apart from road embankments, PVDs will also help to stabilise rail tracks in coastal areas containing a high percentage of clayey subgrades, as demonstrated at Port of Brisbane and Ballina Pacific Highway in Australia. It has also been shown that short PVDs can be used under rail tracks to improve stability by dissipating excess cyclic pore pressure, curtailing lateral displacement, and mitigating mud pumping. Current laboratory observations prove without doubt that high speed trains cannot operate efficiently on tracks built on soft subgrade clays unless it is consolidated before construction, or subjected to alternative improvements such as chemical treatment, stone columns, deep mixing etc. Much of this research is still ongoing worldwide, particularly in view of future high transport networks. In Australia, particular attention to this kind of ground improvement research is given since the government approval of the 2000+ km long Melbourne-to-Brisbane Inland Rail project.

10. ACKNOWLEDGEMENTS

As the 4th Louis Menard Lecturer, my sincere thanks go to all the members of the TC211 (Ground Improvement) of ISSMGE and its Executive Committee, for selecting me for this prestigious presentation. My special thanks are conveyed to Serge Varaksin (former Chair) for his inspiring comments, constructive criticisms and leadership over many years, in the area of soft soil improvement.

I am particular grateful to my colleagues Dr. Rui Zhong, A/Prof Cholachat Rujikiatkamjorn, Dr Mojtaba Kan, Dr Rohan Walker, and Pankaj Baral (PhD student) for their kind help and technical contributions during the preparation of this paper.

Dr Geng Xueyu (now at Warwick University), Vasantha Wijeyakulasuriya (formerly at QLD Main Roads), Dr Richard Kelly (SMEC) and Geoff McIntosh (Douglas Partners) have contributed significantly to my past research through numerous past and present Australian Research Council projects, and to them I owe my sincere appreciation. Without sustained and sufficient funding from the Australian Research Council, much of my research work could not have been made possible.

A number of former doctoral students, including, Dr Wayan Redana (plane strain conversion), Dr Iyathurai Sathananthan (mathematical modelling), Dr Kourosh Kianfar (non-Darcian radial flow), Dr Darshana Perera (soil disturbance), Dr Ni Jing (cyclic soil instability), Dr Ali Ghandeharioon (cavity expansion), Anass Attya (cyclic soil testing), Dr Chamari Bamunawita (numerical modelling), Made Ardana (PVDs installation) and a few current doctoral students (Thanh Trung Nguyen, Kirti Choudhary and Mandeep Singh) have also contributed to the contents and ideas presented herein directly or indirectly.

The support and cooperation received at various times from many colleagues in both academia and practice is gratefully appreciated. While it is impossible to name of all of them, my special thanks are conveyed to Prof. (Bala) Balasubramaniam, Prof Harry Poulos, Prof. Serge Leroueil, Prof John Carter, Prof Chu Jian, Prof. Jian-hua Yin, Prof Scott Sloan, Prof Dave Potts and Prof Kerry Rowe, who have been involved with me in various projects, as well as to Prof. Norbert Morgenstern, Prof Jean-Louis Briaud, A/Prof Hadi Khabbaz, Prof. Dennes Bergado, Prof. Robin Chowdhury, Dr. Jayantha Ameratunga, Prof. Sven Hansbo, Prof Antonio Gens, Tim Neville, Prof Roger Frank, Dave Christie, Prof. Ted Brown, Prof. Peter Kaiser, Patrick Wong, Prof. Chandra Desai, Peter Boyle, Assoc. Prof. (Siva) Sivakugan, Dr Brook Ewers, Henk Buys, Prof. Gholamreza Mesri, Mark Adams, Prof. Dave Chan, Prof Sarah Springman, Cynthia de Bok, Prof. Mohamed Sakr, Prof. Mounir Bouassida, Daniel Berthier, Prof. Pedro Pinto, Prof. Madira Madhav, Prof. Nasser Khalili, Prof. Jinchun Chai, A/Prof Mohammad Shahin, Dr Gamini Adikari, Prof. Maosong Huang, Prof. Brian Uy, Dr Phil Flentje, Prof R. Robinson, Prof. Felix Darve, Julian Gerbino, Bob Armstrong, Michael Thomas, Prof Deepankar Choudhury, Dr. Jayan Vinod, A/Prof Samanthika Liyanapathirana, Dr Martin Liu, Dr Sanjay Nimbalkar, Prof Lijun Su, Dr Sudip Basack, P K Choudhury, Greg Ryan and Lan Ruixue among others for their assistance on various occasions.

I wish to thank a number of technical staff at University of Wollongong, namely, Alan Grant and Cameron Neilson who have been particularly trained in soft soil testing. I also owe my gratitude to Queensland Main Roads, Port of Brisbane Corporation, Roads and Maritime Services (NSW), Coffey Geotechnics, Douglas Partners, SMEC, Menard Bachy, SoilWicks, Sydney Trains, ARTC, National Jute Board (India) and GeoHarbour (China) for their continuous support in terms of research funding and technical assistance during numerous R&D projects over the past two decades.

Much of the contents produced in this paper have been reproduced with kind permission from the Australian Geomechanics Journal (e.g. Author's 2009 EH Davis Lecture), Journal of Geotechnical & Geoenvironmental Engineering ASCE, International Journal of Geomechanics, ASCE, Proceedings of the Institution of Civil Engineers – Ground Improvement, ASTM Geotechnical Testing Journal, Géotechnique and Canadian Geotechnical Journal among others.

11. REFERENCES

Aboshi, H., Sutoh, Y., Toshiyuki, I, And Shimizu, Y 2001. Kinking deformation of PVD under consolidation settlement of surrounding clay. Soils and Foundations 5: 25-32.

Abuel-Naga, H.M., Pender, M.J., Bergado, D.T., 2012. Design curves of prefabricated vertical drains including smear and transition zones effects. Geotextiles and Geomembranes, 32, 1-9.

Akagi, T. 1979. Consolidation caused by mandrel-driven sand drains. Proceedings of the 6th Asian Regional Conference on Soil Mechanics and Foundation Engineering, Singapore, Southeast Asian Geotechnical Society, Bangkok, Vol.1: 125-128.

Araujo, G.L.S., Palmeira, E.M. and Macedo, I.L. 2012. Comparisons between predicted and observed behaviour of a geosynthetic reinforced abutment on soft soil. Engineering Geology, Vol. 147-148: 101-113.

Asha, B.S. and Mandal, J.N. 2012. Absorption and discharge capacity tests on natural prefabricated vertical drains. Geosynthetics International, 19: 263-271.

Asaoka, A. 1978. Observational procedure of settlement prediction. Soils and Foundations 18(4): 87–101.

Azari, B., Fatahi, B., Khabbaz, H. 2016. Assessment of the Elastic-Viscoplastic Behavior of Soft Soils Improved with Vertical Drains Capturing Reduced Shear Strength of a Disturbed Zone. International Journal of Geomechanics 16(1): B4014001.

Barron, R.A. 1948. Consolidation of fine-grained soils by drain wells. Transactions, ASCE, 113: 718-754.

Bari, M.W., Shahin, M.A., 2014. Probabilistic design of ground improvement by vertical drains for soil of spatially variable coefficient of consolidation. Geotext. Geomembr. 42, 1–14.

Basu, D. and Madhav, M. R. 2000. Effect of Prefabricated Vertical Drain Clogging on the Rate of Consolidation: A Numerical Study. Geosynthetics International 7(3): 189-215.

Basu, D., Basu, P., and Prezzi, M. 2006. Analytical solutions for consolidation aided by vertical drains. 1(1): 63-71.

Basu, D. and Prezzi, M. 2007. Effect of the smear and transition zones around prefabricated vertical drains installed in a triangular pattern on the rate of soil consolidation. Int. J. of Geomechanics, 7(1): 34-43.

Basu, D., et al. 2009. Effect of Soil Disturbance on Consolidation By Prefabricated Vertical Drains Installed in a Rectangular Pattern. Geotechnical and Geological Engineering 28(1): 61-77.

Basu, D., Prezzi, M., and Madhav, M.R. 2010. Effect of Soil Disturbance on Consolidation By Prefabricated Vertical Drains Installed in a Rectangular Pattern. Geotechnical and Geological Engineering, 28(1): 61-77.

Bergado, D. T., Asakami, H., Alfaro, M.C., and Balasubramaniam, A.S. 1991. Smear effects of vertical drains in soft Bangkok clay. Geotechnical Engineering, ASCE, 117(10): 1509–1530.

Bergado D.T., Mukherjee K. Alfaro M. C. & Balasubramaniam, A. S. 1993. Prediction of vertical-band-drain performance by the finite-element method. Geotextiles & Geomembranes 12(6): 567-586.

Bergado, D. T., Manivannan, R., Balasubramaniam, A. S. 1996. Proposed criteria for discharge capacity of prefabricated vertical drains. Geotextiles and Geomembranes 14(9): 481-505.

Bergado, D.T., Chai, J.C., Miura, N., Balasubramaniam, A.S., 1998. PVD improvement of soft Bangkok clay with combined vacuum and reduced sand embankment preloading. Geotechnical Engineering, 29, 95–122.

Bergado, D. T., Balasubramaniam, A. S., Fannin, R. J. and Holta, R. D. 2002. Prefabricated vertical drains (PVDs) in soft Bangkok clay: a case study of the new Bangkok International Airport Project, Canadian Geotechnical Journal. 39: 304-315.

Bjerrum, L. 1967. Engineering geology of Norwegian normally-consolidated marine clays as related to settlement of buildings, Geotechnique, 17(2): 73-96.

Bo, MW, Bawajee, R and Choa, V. 1998. Smear effect due to mandrel penetration. Proc. of the 2nd International Conference on Ground Improvement Techniques, CI Premier, Singapore, 83–92.

Bo, M. W., Chu, J., Low, B. K., and Choa, V. 2003. Soil improvement; prefabricated vertical drain techniques, Thomson Learning, Singapore.

Brennan, A. J. and Madabhushi, S.P.G. 2006. Liquefaction remediation by vertical drains with varying penetration depths. Soil Dynamics and Earthquake Engineering 26(5): 469-475.

Carter, J. P., Booker, J. R., and Wroth, C.P. 1980. The Application of a Critical State Soil Model to Cyclic Triaxial Tests. Proc., 3rd Australia-New Zealand Conf. Geomech., Wellington, NZ, 121-126.

Carter, J. P., Booker, J. R., and Wroth, C.P. 1982. A critical state soil model for cyclic loading. Soil mechanics-transient and cyclic loading, Chichester: John Wiley & Sons, 219-252.

Carrillo, N. 1942. Simple two and three-dimensional consolidation. J. Math. Phys. 21(1), 1–5.

Cascone, E. and Biondi, G. 2013. A case study on soil settlements induced by preloading and vertical drains. Geotextiles and Geomembranes 38: 51-67.

Chai, J.C. and Miura, N. 1999. Investigation of Factors Affecting Vertical Drain Behavior. Journal of Geotechnical and Geoenvironmental Engineering 125(3): 216-226.

Chai, J. C., Cater, J. P., and Hayashi, S. 2005. Ground deformation induced by vacuum consolidation. Journal of Geotechnical and Geoenvironmental Engineering, ASCE, 131(12): 1552-1561.

Chai, J. C., Carter, J.P., and Hayashi, S. 2006. Vacuum consolidation and its combination with embankment loading. Canadian Geotechnical Journal 43(10): 985-996.

Chai, J. C., Miura, N., and Bergado, D. T. 2008. Preloading clayey deposit by vacuum pressure with cap-drain: Analyses versus performance. Geotexiles and Geomembranes, 26: 220-230.

Chai, J., Hong, Z. And Shen, S. 2010. Vacuum-drain consolidation induced pressure distribution and ground deformation. Geotextiles and Geomembranes 28(6): 525-535.

Chai, J., Ong, C.Y., Carter, J.P., and Bergado, D.T. 2013. Lateral displacement under combined vacuum pressure and embankment loading. Géotechnique 63(10): 842-856.

Chen, R.P., Zhou, W.H., Wang, H.Z., Chen, Y.M. 2005. One-dimensional nonlinear consolidation of multi-layered soil by differential quadrature method. Computers and Geotechnics, 32(5), 358–369.

Choa, V. 1990. Soil improvement works at Tianjin East Pier project. Proceedings 10th Southeast Asian Geotechnical Conference, Taipei, 1: 47-52.

Choudhary, K., Indraratna, B., and Rujikiatkamjorn C. 2016 Pore pressure based method to quantify smear around a vertical drain Géotechnique Letters 6, 1–5.

Chu, J., Yan, S. W., and Yang, H. 2000. Soil improvement by vacuum preloading method for an oil storage station. Geotechnique, 50(6): 625-632.

Chu, J., and Yan, S.W. 2005a. Application of vacuum preloading method in soil improvement project. Case Histories Book, Edited by Indraratna, B. and Chu, J., Elsevier, London. Vol. 3: 91-118.

Chu, J. and S. Yan (2005b). Estimation of Degree of Consolidation for Vacuum Preloading Projects. International Journal of Geomechanics 5(2): 158-165.

Chu, J., Indraratna, B., Yan, S., Rujikiatkamjorn, C., 2014. Overview of preloading methods for soil improvement. Proc. Inst. Civ. Eng. - Gr. Improv. 167, 173–185. 569.

Chung, S. G., et al. 2009. Hyperbolic Method for Prediction of Prefabricated Vertical Drains Performance. Journal of Geotechnical and Geoenvironmental Engineering 135(10): 1519-1528.

Chung, S. G. and Lee, N. K. 2010. Smear Effect and Well Resistance of PVD-Installed Ground Based on the Hyperbolic Method. Journal of Geotechnical and Geoenvironmental Engineering 136(4): 640-642.

Chung, S.G., Kweon, H.J., Jang, W.Y. 2014. Observational method for field performance of prefabricated vertical drains. Geotext. Geomembr. 42, 405–416.

Cognon, J.M., Juran, I and Thevanayagam, S. 1994. Vacuum consolidation technology – principles and field experience. Proceedings of the Conference on Vertical and Horizontal Deformations of Foundations and Embankments, College Station, TX, USA, (Yeung AT and Felio GY (eds.). ASCE, New York, NY, USA, Geotechnical Special Publication 40, 1237–1248.

Conte, E. and Troncone, A. 2009. Radial consolidation with vertical drains and general time-dependent loading. Canadian Geotechnical Journal 46(1): 25-36.

Deng Y.B., Xie K.H., Lu M.M, Tao H.B. & Liu G.B. 2013. Consolidation by prefabricated vertical drains considering the time dependent well resistance. Geotextiles & Geomembranes,36:20-26.

Fang, Z. and Yin, J.H. 2006. Physical modelling of consolidation of Hong Kong marine clay with prefabricated vertical drains. Canadian Geotechnical Journal 43(6): 638-652.

Fox, P. J., Di Nicola, M., and Quigley, D. W. 2003. Piecewise-linear model for large strain radial consolidation. Journal of Geotechnical and Geoenvironmental Engineering, 129(10): 940–950.

Gabr M.A., and Szabo D.J. 1997. Prefabricated vertical drains zone of influence under vacuum in clayey soil. Conference on In Situ Remediation of the Geoenvironment, ASCE: 449-460.

Geng, X., et al. 2011. Effectiveness of partially penetrating vertical drains under a combined surcharge and vacuum preloading. Canadian Geotechnical Journal 48(6): 970-983.

Geng X.Y., Indraratna B., and Rujikiatkamjorn C. 2012. Analytical Solutions for a Single Vertical Drain with Vacuum and Time-Dependent Surcharge Preloadingin Membrane and Membraneless Systems. Int. Journal of Geomechanics, ASCE, 12(1): 27-42.

Ghandeharioon, A., Indraratna, B., and Rujikiatkamjorn, C. 2010. Analysis of soil disturbance associated with mandrel-driven prefabricated vertical drains using an elliptical cavity expansion theory. Int. J. Geomech., 10(2), 53–64.

Hansbo, S. 1979. Consolidation of clay by band-shaped prefabricated drains. Ground Engineering, 12(5): 16-25.

Hansbo, S. 1981. Consolidation of fine-grained soils by prefabricated drains and lime column installation. In Proceedings of 10th International Conference on Soil Mechanics and Foundation Engineering, Stockholm, A.A. Balkema, Rotterdam, The Netherlands. Vol. 3,677-682.

Hansbo, S. 1987. Fact and fiction in the field of vertical drainage. In Prediction and performance in geotechnical engineering (eds R. J. Joshi & F. G. Griffiths). Rotterdam/Boston: Balkema.

Hansbo, S. 1997. Aspects of vertical drain design: Darcian or non-Darcian flow. Géotechnique, 47(5): 983-992.

Hird C.C., Pyrah I.C., and Russel D. 1992. Finite element modeling of vertical drains beneath embankments on soft ground. Geotechnique, 42(3): 499-511.

Hird, C.C., Pyrah, I.C., Russell, D. and Cinicioglu, F. 1995. Modelling the effect of vertical drains in two-dimensional finite element analyses of embankments on soft ground. Canadian Geotechnical Journal, 32, 795-807

Ho, L., Fatahi, B., Khabbaz, H. 2014. Analytical solution for one-dimensional consolidation of unsaturated soils using eigenfunction expansion method. Int. J. Numerical and Analytical Methods in Geomechanics, 38, 1058–1077.

Ho, L., Fatahi, B., Khabbaz, H. 2015. A closed form analytical solution for two- dimensional plane strain consolidation of unsaturated soil stratum. Int. J. Numer. Anal. Methods Geomech. 39, 1665–1692.

Ho, L., and Fatahi, B. 2016. One-dimensional consolidation analysis of unsaturated soils subjected to time-dependent loading. Int. J. Geomech. 16, 1–19.

Ho, L., Fatahi, B., Khabbaz, H., 2016. Analytical solution to axisymmetric consolidation in unsaturated soils with linearly depth-dependent initial conditions. Comput. Geotech. 74, 102–121.

Holtan, G.W. 1965. Vacuum stabilization of subsoil beneath runway extension at Philadelphia International Airport. Proc. of 6th ICSMFE, Montreal, Vol. 2.: 61-65

Holtz, R.D., Wager, O., 1975. Preloading by vacuum: current prospects. Transport Res. Rec. 588 548, 26–29.

Holtz, R.D., Jamiolkowski, M., Lancellotta, R. & Pedroni, S. 1989 Behaviour of Bent PVDs, Proceedings of 12th ICSMFE, Rio De Janerio, Vol. 3, pp 1657-1660.

Holtz, R.D., Jamiolkowski, M., Lancellotta, R., and Pedroni, R. 1991. Prefabricated vertical drains: design and performance. CIRIA Ground Engineering Report: Butterworth-Heinemann, Oxford.

Howell, R., Rathje, E.M., Kamai, R., and Boulanger, R. 2012. Centrifuge Modeling of Prefabricated Vertical Drains for Liquefaction Remediation. Journal of Geotechnical and Geoenvironmental Engineering 138(3): 262-271.

Hu, Y. Y., Zhou, W. H., and Cai, Y. Q. 2014. Large-strain elastic viscoplastic consolidation analysis of very soft clay layers with vertical drains under preloading. Canadian Geotechnical Journal, 51(2): 144-157.

Indraratna, B., Balasubramaniam, A. S. and Balachandran, S. 1992. Performance of test embankment constructed to failure on soft marine clay. J. of Geotechnical Engineering, ASCE, 118(1): 12-33.

Indraratna, B., Balasubramaniam, A. S., and Ratnayake, P. 1994. Performance of embankment stabilized with vertical drains on soft clay. Journal of Geotechnical Engineering, ASCE, 120(2): 257-273.

Indraratna, B., and Redana, I. W. 1997. Plane strain modeling of smear effects associated with vertical drains. Journal of Geotechnical Engineering, ASCE, 123(5), 474-478.

Indraratna, B., and Redana, I. W. 1998. Laboratory determination of smear zone due to vertical drain installation. Journal of Geotechnical Engineering, ASCE, 125(1): 96-99.

Indraratna, B., and Redana, I. W. 2000). Numerical modeling of vertical drains with smear and well resistance installed in soft clay. Canadian Geotechnical Journal, 37: 132-145.

Indraratna, B., Bamunawita, C., and Khabbaz, H. 2004. Numerical modeling of vacuum preloading and field applications. Canadian Geotechechnical Journal, 41: 1098-1110.

Indraratna, B., Rujikiatkamjorn C., and Sathananthan, I. 2005a. Analytical and numerical solutions for a single vertical drain including the effects of vacuum preloading. Canadian Geotechnical Journal, 42: 994-1014.

Indraratna, B., Sathananthan, I., Rujikiatkamjorn C. and Balasubramaniam, A. S. 2005b. Analytical and numerical modelling of soft soil stabilized by PVD incorporating vacuum preloading. Int. Journal of Geomechanics, ASCE, 5(2): 114-124.

Indraratna, B., Rujikiatkamjorn C., Balasubramaniam. A. S. and Wijeyakulasuriya, V. 2005c. Predictions and observations of soft clay foundations stabilized with geosynthetic drains vacuum surcharge. Ground Improvement - Case Histories Book (volume 3), Edited by Indraratna, B. and Chu, J., Elsevier, London: 199-230.

Indraratna, B., Rujikiatkamjorn, C., and Sathananthan I. 2005d. Radial consolidation of clay using compressibility indices and varying horizontal permeability. Canadian Geotech. Journal 42:1330-1341.

Indraratna, B. and Chu, J. eds 2005e. Ground Improvement Case Histories. Elsevier, Amsterdam

Indraratna, B, Rujikiatkamjorn C and Wijeyakulasuriya, V, Soft clay stabilization using prefabricated vertical drains and the role of viscous creep at the site of sunshine motorway, Queensland, in Proceedings of 10th Australia New Zealand Conference on Geomechanics, Brisbane, Australia, Vol.2, 96-101.

Indraratna, B., and Rujikiatkamjorn, C. 2008. Effects of partially penetrating prefabricated vertical drains and loading patterns on vacuum consolidation. In K. R. Reddy, M. V. Khire and A. N. Alshawabkeh (Eds.), GeoCongress (pp. 596-603). USA: ASCE.

Indraratna, B., Attya, A., and Rujikiatkamjorn, C. 2009. Experimental investigation on effectiveness of a vertical drain under cyclic loads. Journal of Geotechnical and Geoenvironmental Engineering, ASCE, 135 (6): 835-839.

Indraratna, B. 2010. 2009 EH Davis Memorial Lecture: Recent advances in the application of vertical drains and vacuum preloading in soft soil stabilization. Australian Geomechanics Journal, AGS, 45(2), 1-43.

Indraratna, B., Rujikiatkamjorn, C. Adams, M., and Ewers, B., 2010. Class A prediction of the behaviour of soft estuarine soil foundation stabilised by short vertical drains beneath a rail track. Journal of Geotechnical and Geoenvironmental Engineering, ASCE, 136(5), 686-696.

Indraratna, B., Rujikiatkamjorn, C., Ameratunga, J., and Boyle, P. 2011. Performance and Prediction of Vacuum Combined Surcharge Consolidation at Port of Brisbane, Journal of Geotechnical and Geoenvironmental Engineering, ASCE, 137(11): 1009-1018.

Indraratna, B., Rujikiatkamjorn, C., Kelly, R., and Buys, H. 2012. Soft soil foundation improved by vacuum and surcharge loading. Proceedings of the ICE - Ground Improvement 165, 87-96.

Indraratna, B., Rujikiatkamjorn, C., and Balasubramaniam, A. 2014. Consolidation of Estuarine Marine Clays for Coastal Reclamation Using Vacuum and Surcharge Loading. From Soil Behavior Fundamentals to Innovations in Geotechnical Eng.: 358-369.

Indraratna, B., Perera, D., Rujikiatkamjorn, C. & Kelly, R. 2015a. Soil disturbance analysis due to vertical drain installation. Proceedings of the Institution of Civil Engineers: Geotechnical Engineering, 168 (3), 236-246.

Indraratna, B., Ni, J., Rujikiatkamjorn, C., Zhong, R. 2015b. A partially drained model for soft soils under cyclic loading considering cyclic parameter degradation. Australian Geomech. Journal, 50(4), 89-95.

Indraranata, B., Chu, J., Rujikiatkamjorn, C, eds. 2015c. Ground Improvement Case-Histories: Embankments with Special Reference to Consolidation and Other Physical Methods. 1 edition. Butterworth-Heinemann, 2015.

Indraratna, B., Kan, M. E., Potts, D., Rujikiatkamjorn, C. & Sloan, S. W. 2016a. Analytical solution and numerical simulation of vacuum consolidation by vertical drains beneath circular embankments. Computers and Geotechnics, 80 83-96.

Indraratna, B., Nguyen T.T., Carter, J and Rujikiatkamjorn 2016b. Influence of biodegradable natural fibre drains on the radial consolidation of soft soil. Computers & Geotechnics, 78: 171-180.

Indraratna, B., Zhong, R., Fox, P., and Rujikiatkamjorn, C. 2016c. Large-Strain Vacuum-Assisted Consolidation with Non-Darcian Radial Flow Incorporating Varying Permeability and Compressibility. J. Geotech. Geoenviron. Eng. , 10.1061/(ASCE)GT.1943-5606.0001599 , 04016088.

Ing, T.C. and Nie, X.Y. 2002. Coupled consolidation theory with non-Darcian flow. Computers and Geotechnics 29(3): 169-209.

Jacob, A., Thevanayagam, S. and Kavazajian, E., 1994. Vacuum-assisted consolidation of a hydraulic landfill. Vertical and Horizontal Deformations of Foundations and Embankments, Settlement, 94, College Station. Geotechnical Special Publications No 40, ASCE: 1249-1261.

Jamiolkowski, M., Lancellotta, R., and Wolski, W. 1983. Precompression and speeding up consolidation. Proc. 8th ECSMFE: 1201-1206.

Jang, Y.S, Kim, Y.W., and Park, J.Y. 2001. Consolidation efficiency of natural and plastic geosynthetic band drains. Geosynthetics International, 8(4): 283-301.

Johnson, S. J., 1970. Precompression for improving foundation soils. J. of the Soil Mechanics & Foundations Division, ASCE, 1: 111-114.

Karim, M. R. and Lo, S. C. R. 2015. Estimation of the hydraulic conductivity of soils improved with vertical drains. Computers and Geotechnics, 63: 299-305.

Kianfar, K., Indraratna, B. and, Rujikiatkamjorn, C. 2013. Radial consolidation model incorporating the effects of vacuum preloading and non-Darcian flow. Géotechnique, 63: 1060-1073.

Kim, J.H. and Cho, S.D. 2009. Pilot scale field test for natural fiber drain. In Geosynthetics in civil and environmental engineering. Edited by G. Li, Chen, Y. & Tang, X. Springer, 409-414.

Kim, R., Hong, S.J., Lee, M.J. and Lee, W. 2011. Time dependent well resistance factor of PVD. Marine Georesources & Geotechnology, 29(2): 131-144. doi: 10.1080/1064119x.2010.525145.

Kjellman W. 1952, Consolidation of clayey soils by atmospheric pressure. Proceedings of a Conference on Soil Stabilisation, MIT, Boston, pp. 258–263.

Lam, L. G., Bergado, D.T., and Hino, T. 2015. PVD improvement of soft Bangkok clay with and without vacuum preloading using analytical and numerical analyses. Geotextiles and Geomembranes 43(6): 547-557.

Lawrence, C.A. and Koerner, R.M., 1988. Flow Behavior of Kinked Strip Drains,Geosynthetics for Soil Improvement, Holtz, R.D., Editor, ASCE Geotechnical Special Publication No. 18, Proceedings of a symposium held in Nashville, Tennessee, 22-39

Lee, S.L., Ramaswamy, S.D., Aziz, M.A., Das Gupta, N.C. and N. C. & Karunaratne, G.P. 1987. Fibredrain for consolidation of soft soils. Post-Vienna Conference on Geotextiles, Singapore. Vol.2, 238-258

Lee, S.L., Karunaratne, G.P., Ramaswamy, S.D., Aziz, M.A. and Das Gupta, N.C. 1994. Natural geosynthetic drain for soil improvement. Geotextiles and Geomembranes, 13(6–7): 457-474.

Lee, P.K.K., Xie, K.H., 1996. Consolidation characteristics of layered soil installed with vertical drains, in: Proceedings of the 2nd Int. Conference on Soft Soil Engineering. Nanjing, 391–397.

Lei, G.H., Fu, C.W. , Ng, C.W.W. 2016. Vertical-drain consolidation using stone columns: An analytical solution with an impeded drainage boundary under multi-ramp loading, Geotextiles and Geomembranes, 44(1): 122-131.

Lei, G.H., Zheng, Q., Ng, C.W.W., Chiu, A.C.F. & Xu, B. (2015). An analytical solution for consolidation with vertical drains under multi-ramp loading. Géotechnique. Vol. 65, No.7, 531-547.

Leo, C.J. 2004. Equal Strain Consolidation by Vertical Drains. J. of Geotechnical & Geoenvironmental Eng., ASCE 130(3): 316-327.

Leong, E. C., Soemitro, R.A.A. and Rahardjo, H. 2000. Soil improvement by surcharge and vacuum preloadings. Géotechnique 50(5): 601-605.

Liu, H.L. and Chu, J. 2009. A new type of prefabricated vertical drain with improved properties. Geotextiles and Geomembranes 27(2): 152-155.

Liu, J.C., Lei, G.H., Zheng, M.X., 2014. General solutions for consolidation of multilayered soil with a vertical drain system. Geotext. Geomembr. 42, 267–276. 611

Long, P. V., Bergado, D. T., Nguyen, L.V. and Balasubramaniam, A.S. 2013. Design and performance of soft ground improvement using PVD with and without vacuum consolidation. Geotechnical Engineering Journal of the SEAGS & ASGGEA.

Lu, M., Wang, S.Y., Sloan, S., et al. 2015. Nonlinear radial consolidation of vertical drains under a general time-variable loading. International Journal for Numerical and Analytical Methods in Geomechanics 39(1): 51-62.

Lu, M., Wang, S.Y., Sloan, S., et al. 2015. Nonlinear consolidation of vertical drains with coupled radial–vertical flow considering well resistance. Geotextiles and Geomembranes 43(2): 182-189.

Madhav, M.R., Park, Y.M., Miura, N. 1993. Modelling and study of smear zones around band shaped drains. Soils and Foundations, 33(4):135–147.

Marinucci, A. 2010. Effect of prefabricated vertical drains on pore water pressure generation and dissipation in liquefiable sand. The University of Texas at Austin.

Marinucci, A., Rathje, E., Kano, S., Kamai, R., Conlee, C., Howell, R., Boulanger, R., and Gallagher, P. 2008. Centrifuge Testing of Prefabricated Vertical Drains for Liquefaction Remediation. Geotechnical Earthquake Engineering and Soil Dynamics IV: pp. 1-10. doi: 10.1061/40975(318)100.

Mesri, G and Castro, A. 1987. The Cα/Cc concept and K0 during secondary compression, Journal of Geotechnical Engineering, ASCE, 113(3): 230-247.

Mesri, G., Stark, T.D., Ajlouni, M.A. and Chen, C.S. 1997. Secondary compression of peat with or without surcharging. ASCE Journal of Geotechnical Engineering 123(5): 411–420.

Mesri, G. and Khan, A. 2012. Ground improvement using vacuum loading together with vertical drains. Journal of Geotechnical and Geoenvironmental Engineering 138(6): 680-689.

Mesri, G. and Funk, J. 2014. Settlement of the Kansai International Airport Islands. Journal of Geotechnical and Geoenvironmental Engineering, 10.1061/(ASCE)GT.1943-5606.0001224, 04014102.

Miller, G. A., Teh, S. Y., Li, D., and Zaman, M. M. 2000. Cyclic shear strength of soft railroad subgrade. J. Geotech. Geoenviron. Eng., 126(2), 139-147.

Mirjalili, M., Kimoto, S., Oka, F., and Hattori, T. 2012. Long-term consolidation analysis of a large-scale embankment construction on soft clay deposits using an elasto-viscoplastic model. Soils and Foundations 52(1): 18-37.

Miura, T., M, T., H, M. and M, B. 1995. The basic experiment on permeability characteristics of fibredrain. Proceeding of Annual Regional Meeting of JSCE. Kyushu (in Japanese).

Mohamedelhassan E., and Shang, J.Q. 2002. Vacuum and surcharge combined one-dimensional consolidation of clay soils, Canadian Geotechnical Journal, 39: 1126-1138.

Nash, D.F.T. and Ryde, S. J. 2001. Modelling consolidation accelerated by vertical drains in soils subject to creep. Géotechnique 51(3): 257-273.

Nguyen, T. T. and B. Indraratna 2016. Experimental and numerical investigations into hydraulic behaviour of coir fibre drain. Canadian Geotechnical Journal, 10.1139/cgj-2016-0182.

Ni, J., Indraratna, B., Geng, X.Y. 2013. Radial consolidation of soft soil under cyclic loads. Computers and Geotechnics 50: 1-5.

Ni, J., Indraratna, B., Geng, X. Y., Carter, J. P. and Chen, Y. L. 2015. Model of soft soils under cyclic loading. Int. J. of Geomechanics, 15(4): 04014067 1-10

Ong C.Y., Chai J.C. and Hino, T. 2012. Degree of consolidation of clayey deposit with partially penetrating vertical drains. Geotextiles and Geomembranes 34(5): 19–27.

Onoue, A. 1988. Consolidation by vertical drains taking well resistance and smear into consideration. Soils & Foundations, 28(4): 165-174.

Parsa-Pajouh, A., Fatahi, B., Vincent, P., and Khabbaz, H. 2014. Trial Embankment Analysis to Predict Smear Zone Characteristics Induced by Prefabricated Vertical Drain Installation. Geotechnical and Geological Engineering 32(5): 1187-1210.

Qian, J.H., Zhao, W.B., Cheung, Y.K. and Lee, P.K.K. 1992. The theory and practice of vacuum preloading. Computers and Geotechnics, 13: 103-118.

Razouki, S. S. 2016. Radial consolidation clay behaviour under haversine cyclic load. Proceedings of the Institution of Civil Engineers - Ground Improvement, 169(2): 143-149.

Richart F.E. 1957. A review of the theories for sand drains. Journal of the Soil Mechanics and Foundations Division, ASCE, 83(3): 1-38.

Robinson, R. G., et al. 2012. Final state of soils under vacuum preloading. Canadian Geotechnical Journal 49(6): 729-739.

Rujikiatkamjorn, C., Indraratna, B. 2007. Analytical solutions and design curves for vacuum-assisted consolidation with both vertical and horizontal drainage, Canadian Geotech. Journal, 44: 188-200.

Rujikiatkamjorn, C., Indraratna, B. N. and Chu, J. 2008. 2D and 3D numerical modeling of combined surcharge and vacuum preloading with vertical drains. Int. J. Geomechanics, ASCE, 8(2): 144-156.

Rujikiatkamjorn, C. Ardana, M., Indraratna, B., and Leroueil, S. 2013. Conceptual Model Describing Smear Zone Caused by Mandrel Action. Géotechnique. 63(16): 1377-1388.

Rujikiatkamjorn, C. and Indraratna, B. 2014a. Analytical Solution for Radial Consolidation Considering Soil Structure Characteristics, Canadian Geotechnical Journal. 52(7): 947-960.

Rujikiatkamjorn, C., Indraratna, B., 2014b. Environmental Sustainability of Soft Soil Improvement via Vacuum and Surcharge Preloading, Geo-Congress, ASCE, 3658–3665.

Saha, P., Roy, D., Manna, S., Adhikari, B., Sen, R. and Roy, S. 2012. Durability of transesterified jute geotextiles. Geotextiles and Geomembranes, 35: 69-75. doi: http://dx.doi.org/10.1016/j.geotexmem.2012.07.003.

Saowapakpiboon, J., Bergado, D.T., Youwai, S., Chai, J.C., Wanthong, P., and Voottipruex, P. 2010. Measured and predicted performance of prefabricated vertical drains (PVDs) with and without vacuum preloading. Geotextiles and Geomembranes 28(1): 1-11.

Saowapakpiboon, J., et al. 2011. PVD improvement combined with surcharge and vacuum preloading including simulations. Geotextiles and Geomembranes 29(1): 74-82.

Sathananthan, I. and Indraratna, B. 2006. Laboratory evaluation of smear zone and correlation between permeability and moisture content. Journal of Geotechnical and Geoenvironmental Engineering, ASCE, 132(7):1090-0241.

Sathananthan, I., Indraratna, B. N. and Rujikiatkamjorn, C. 2008. Evaluation of smear zone extent surrounding mandrel driven vertical drains using the cavity expansion theory. International Journal of Geomechanics, 8 (6): 355-365.

Saye, S. R. 2001. Assessment of soil disturbance by the installation of displacement sand drains and prefabricated vertical drains. Soil Behaviour and Soft Ground Construction, Geotechnical Special Publication No. 119: 325-362. Reston, VA: ASCE.

Seah, T.H. 2006. Design and construction of ground improvement works at Suvarnabhumi Airport. Geotechnical Engineering Journal of the Southeast Asian Geotechnical Society, 37: 171-188.

Shang, J.Q., Tang, M., Miao, Z., 1998. Vacuum preloading consolidation of reclaimed land: a case study. Canadian Geotechnical Journal, 35, 740–749.

Sharma, J.S. and Xiao, D. 2000. Characterization of a smear zone around vertical drains by large-scale laboratory tests. Canadian Geotechnical Journal 37(6): 1265–1271.

Shen, S.L., Chai, J.C., Hong, Z.S., Cai, F.X., 2005. Analysis of field performance of embankments on soft clay deposit with and without PVD-improvement. Geotext. Geomembr. 23, 463–485.

Tang, X.W., Onitsuka, K., Xie, K.H., 1997. Consolidation solution for double-layered ground with vertical ideal drains, in: Proceedings of the 9th Int. Conf. of the Association for Computer Methods and Advances in Geomechanics. Wuhan, pp. 447–450.

Tang, M. and J. Q. Shang 2000. Vacuum preloading consolidation of Yaoqiang Airport runway. Ground and Soil Improvement: 9-19.

Tang, X.W., Onitsuka, K., 2001. Consolidation of double-layered ground with vertical drains. Int. J. Numer. Anal. Methods Geomech. 25, 1449–1465.

Tran, T.A. and Mitachi, T. 2008. Equivalent plane strain modelling of vertical drains in soft ground under embankment combined with vacuum preloading. Computers and Geotechnics 35(5): 655–672.

Venda Oliveira, P. J. and Lemos, L. J. L. 2011. Numerical analysis of an embankment on soft soils considering large displacements. Computers and Geotechnics 38(1): 88-93.

Voottipruex, P., Bergado, D., Lam L. & Hino, T. (2014). Back-analyses of flow parameters of PVD improved soft Bangkok clay with and without vacuum preloading from settlement data and numerical simulations. Geotextiles & Geomembranes, 42(5): 457-467.

Walker, R. and Indraratna, B. 2006. Vertical drain consolidation with parabolic distribution of permeability in smear zone. Geotechnical and Geoenvironmental Engineering, ASCE, 132(7), 937-941.
Walker, R. and Indraratna, B. 2007. Vertical drain consolidation with overlapping smear zones. Geotechnique, 57 (5): 463-467.
Walker, R., Indraratna, B., 2009. Consolidation analysis of a stratified soil with vertical and horizontal drainage using the spectral method. Géotechnique 59, 439–449.
Walker, R. T. 2011. Vertical drain consolidation analysis in one, two and three dimensions. Computers & Geotechnics 38(8): 1069-1077.
Walker, R., Indraratna, B. and Rujikiatkamjorn, C. 2012. Vertical drain consolidation with non-darcian flow and void ratio dependent compressibility and permeability, Géotechnique, 62(11), 985-997.
Wang, X.S., Jiao, J.J., 2004. Analysis of soil consolidation by vertical drains with double porosity model. Int. J. Numer. Anal. Methods Geomech. 28, 1385–1400.
Wijeyakulasuriya, V., Hobbs, G., and Brandon, A. 1999. Some experiences with performance monitoring of embankments on soft clays. Proc., 8th Australia New Zealand Conf. on Geomechnics, Vol. 2, Australian Geomechanics Society, Hobart, 783–788.
Wu, T.H., Zhou, S.Z., and Gale, S.M. 2007. Embankment on sludge: predicted and observed performances. Canadian Geotechnical Journal 44(5): 545-563.
Xie, K.H., and Leo, C. J. 2004. Analytical solutions of one-dimensional large strain consolidation of saturated and homogeneous clays. Computers and Geotechnics, 31(4): 301-314.
Xu, B., Yang, J., Noda, T., 2015. Finite element analysis of soft ground improvement by vacuum preloading combined with surcharge preloading. 6th Japan-China Geotech. Symp. 1, 1–5.
Yan, S.W. and Chu, J. 2003. Soil improvement for a road using a vacuum preloading method. Ground Improvement, 7(4): 165-172.
Yan, S. W. and Chu, J. 2005. Soil improvement for a storage yard using the combined vacuum and fill preloading method. Canadian Geotechnical Journal 42(4): 1094-1104.
Ye, G., Zhang, Z., Han, J., et al. 2012. Performance evaluation of an embankment on soft soil improved by deep mixed columns and prefabricated vertical drains. Journal of Performance of Constructed Facilities 27(5): 614-623.
Yildiz, A., Karstunen, M., Krenn, H. 2009. Effect of Anisotropy and Destructuration on Behavior of Haarajoki Test Embankment. International Journal of Geomechanics 9(4): 153-168.
Yin, J. H. and Clark, J. I. 1994. One-dimensional time dependent stress-strain behaviour of soils, elastic visco-plastic modelling, and consolidation analysis (Part 1). The Journal of Rock and Soil Mechanics, the Chinese Academy of Sciences, 15(3): 65-80, (in Chinese). Part 2 on 15(4): 65-75 (in Chinese).
Yin, J. H. and J. Graham 1988. Viscous–elastic–plastic modelling of one-dimensional time-dependent behaviour of clays. Canadian Geotechnical Journal, 1989, 26(2): 199-209.
Yun, T.K. and Leroueil, S. 2001 Modeling the viscoplastic behaviour of clays during consolidation: Application to Berthierville clay in both laboratory and field conditions. Can.Geot. J. 38(3): 484–497.
Zeng, G.X., Xie, K.H., 1989. New development of the vertical drain theories, Proc. 12th ICSMFE. Rio de Janeiro, 1435–1438.
Zhou, J., and Gong, X. 2001. Strain degradation of saturated clay under cyclic loading. Can. Geotech. J., 38(1), 208–212.
Zhou, W.H., Zhao, L.S., 2013. One-dimensional consolidation of unsaturated soil subjected to time-dependent loading with various initial and boundary conditions. Int. J. Geomech. 14, 291–301.
Zhou, W.H., 2013. Axisymmetric consolidation of unsaturated soils by differential quadrature method. Math. Probl. Eng. 2013.
Zhu, G. F., and Yin, J. H. 2004. Consolidation analysis of soil with vertical and horizontal drainage under ramp loading considering smear effects. Geotextiles and Geomembranes, 22(1-2): 63-74.